A microprobe study of tephra glasses from the Fjallsendahraun lava, central Iceland

Ingibjörg Þórðardóttir

Faculty of Earth Science
University of Iceland
2020

A microprobe study of tephra glasses from the Fjallsendahraun lava, central Iceland

Ingibjörg Þórðardóttir

10 ETCS thesis submitted in partial fulfilment of
Baccalaureus Scientiarum degree in Geology

Advisor
Sæmundur Ari Halldórsson
Associate research professor

Faculty of Earth Science
School of Engineering and Natural Sciences
University of Iceland
Reykjavík, June 2020

A microprobe study of tephra glasses from the Fjallsendahraun lava, central Iceland
A microprobe study of the Fjallsendahraun lava
10 ETCS thesis submitted as partial fulfilment of *Baccalaureus Scientiarum* degree in Geology

Faculty of Earth Science
School of Engineering and Natural Sciences
University of Iceland
Askja, Sturlugata 7
101 Reykjavík

Telephone: 525 4000

Registration information:
Ingibjörg Þórðardóttir, 2020, *A microprobe study of tephra glasses from the Fjallsendahraun lava, central Iceland*, BSc thesis, Faculty of Earth Science, University of Iceland, 53 pp.

Printing: Háskólaprent
Reykjavík, June 2020

Abstract

The ~1362 A.D Fjallsendahraun lava in central Iceland originates from the Bárðarbunga volcanic system. Bárðarbunga is one of the youngest and most active volcanic system in Iceland with over 20 known basaltic eruptions in historical time. In this study, major element analysis of 16 glassy tephra samples from recent basaltic fissure eruptions which all originated within the Bárðarbunga system are presented. The samples come from Fjallsendahraun (11), Tjörvahraun (1), Tröllahraun (2), Vatnaöldur (1) and Veiðivötn (1). Additional datasets from four other localities, including the recent 2014-15 Holuhraun, are used for comparison. All sample localities apart from Tjörvahraun are basaltic in composition and display compositions typical for fissure lavas erupted in central Iceland. Fjallsendahraun is compositionally indistinguishable from other historical basalts from the Bárðarbunga volcanic system, suggesting that these lava units all originate from a shared mid-crustal magma body. Furthermore, the estimated pressure (or depth) of this suggested magma body is ~1,8 kbar.

Útdráttur

Fjallsendahraun (~1362 e.kr) er staðsett vestan við Öskju á mið-Íslandi og á uppruna sinn að rekja til megineldstöðvarinnar Bárðarbungu. Bárðarbunga er ein elsta og virkasta megineldstöð Íslands og hefur framkvæmt rúmlega 20 flæðigos á sögulegum tíma. Þessi rannsókn inniheldur efnagreiningar á aðalefnum úr 16 glersýnum frá Fjallsendahrauni (11), Tjörvahrauni (1), Tröllahrauni (2), Vatnaöldum (1) og Veiðivötnum (1). Hraunin eru tiltölulega nýleg og með sameiginlegan uppruna í Bárðarbungu. Að auki eru efnagreiningar frá fjórum öðrum hraun- og gjóskueiningum notaðar til samanburðar, meðal annars Holuhraun 2014-15. Allar hrauneiningarnar fyrir utan Tjörvahraun eru basískar með dæmigerða efnasamsetningu fyrir flæðigos á mið-Íslandi. Fjallsendahraun er efnafræðilega óaðgreinanlegt frá öðrum sögulegum hrauneiningum úr Bárðarbungu sem bendir til þess að hraunin eiga sameiginlegan uppruna í frumstæðan kvikugeymi í miðri skorpunni. Álykt aður þrýstingur (eða dýpi) á kvikugeyminum er ~1,8 kbar.

Table of Contents

List of figures

List of tables

Abbreviations

BP – Before Present, 1950

BSE – Back-scatter Electron

cm – Centimeter

cpx - Clinopyroxene

EPMA – Electron Probe Micro Analysis

ERZ – Eastern Rift Zone

km – Kilometer

lld – Liquid line of descent

μm - Micrometer

mm - Millimeter

Myr – Million years

MAR – Mid-Atlantic Ridge

Vol% - Volume percent

Wt% – Weight percent

Acknowledgements

I want to thank my advisor Sæmundur Ari Halldórsson who suggested this project for me and was always there to help, despite a busy schedule and a global pandemic.

I thank Alberto Caracciolo and Rebekka Hlín Rúnarsdóttir for the guidance and assistance in the lab, I thank Guðmundur Heiðar Guðfinnsson for helping me with the microprobe analysis and last but not least I thank Enikő Bali for helping me with last minute calculations.

1 Introduction

Bárðarbunga is an active volcanic system within the Eastern Rift Zone (ERZ) in central Iceland. Located beneath the Vatnajökull icecap, the Bárðarbunga central volcano is thought to lie directly above the center of the Iceland magma plume and spreads out in two directions to create a 190 km long fissure swarm (Thordarson & Höskuldsson, 2008). Volcanic activity is largely characterized by basaltic fissure eruptions that can last from hours to a few years. The Bárðarbunga volcanic system has erupted 23 times in historical time (Thordarson & Larsen, 2007).

Previous studies reveal that historic lavas from the Bárðarbunga volcanic system are nearly identical in chemical composition (e.g. Jakobson, 1979; Halldórsson et al., 2018; Caracciolo et al., 2020). The well-documented Holuhraun 2014-15 lava is the most recent addition to Bárðarbunga lavas and it also proved to be nearly indistinguishable in terms of composition compared to previous historical lavas. This lack of compositional variability between lava units is thought to be the result of a shared magma reservoir or body underneath the volcanic system that feeds all the basaltic fissure eruptions spanning the 190 km long fissure swarm (Halldórsson et al., 2018).

The ~1382 A.D Fjallsendahraun lava was formed in a fissure eruption which occurred at the northern part of the volcanic system, close to the subglacially erupted Dyngjufjöll Ytri hyaloclastite ridge (e.g. Sigvaldason, 1992). While of significant volume, this lava unit has received rather little attention and as a result, this study aims to shed light on the geochemical composition of the Fjallsendahraun lava and compare it to other well-documented historical lavas from the Bárðarbunga volcanic system with specific regard to the well-documented Holuhraun 2014-15 eruption. Compositional trends between lava units are compared using tephra glass samples which may represent the liquid melt compositions. Furthermore, petrological data consisting of BSE images from several sample localities are presented along with normative mineralogy and thermobarometry interpretations to further compare similarities between lava units and conceptualize a supposed magma body.

2 Background and geological setting

2.1 Central Iceland: Petrological framework

Iceland is a volcanic island situated on the Mid-Atlantic Ridge where a hot upwelling mantle plume lies beneath. This creates a unique geological setting where a mantle plume merges with a divergent boundary, generating the substantial volcanic activity present in Iceland (Maclennan et al., 2003). Iceland is relatively young on a geological timescale. Ranging from 15-16 Myr, the oldest bedrock above sea level is found on the outermost coast of NW and SE Iceland, parallel to the Mid-Atlantic Ridge which runs across Iceland in a NE-SW direction. Volcanic activity in Iceland is usually limited to one or few volcanic zones at a time. The volcanic zones are created at the center of the island above the mantle plume and as a result of rifting processes new bedrock is created and spread in both directions perpendicular to the MAR. The 15-16 Myr bedrock found in NW and SE Iceland was originally the same bedrock unit making up the former center of the island (e.g. Jóhannesson, 1980; Einarsson, 2008).

Areas of volcanic activity in Iceland are categorized into volcanic zones for example the Eastern Rift Zone and Northern Rift Zone (Figure 1) which are characterized and recognized by their geochemical and petrographical make-up as well as specific patterns in regional tectonics. Volcanic zones consist of one or several volcanic systems for example Bárðarbunga, Torfajökull and Grímsvötn which are all part of the ERZ. Volcanic systems consist of a fissure swarm with an accompanying central volcano and in some cases a summit crater or caldera (e.g. Jóhannesson, 1980; Thordarson & Höskuldsson, 2008).

The Eastern Rift Zone is the most recent volcanic system in Iceland. It has a distinct petrochemical gradient meaning that the chemical composition of rock formations changes depending on locality (Jakobsson, 1979). Three volcanic rock series have developed in Iceland, those are the tholeiitic, alkalic and transitional alkalic series. Rock formations in the ERZ are tholeiitic in the northeast close to Bárðarbunga, with high Fe and Ti content and relatively low Al content. Moving further southwest, in Vestmanneyjar, the ERZ rock formations are alkalic, characterized by the relatively high alkali (K_2O+Na_2O) content (Jakobsson, Jónasson & Sigurðsson, 2008; Jakobsson, 1979).

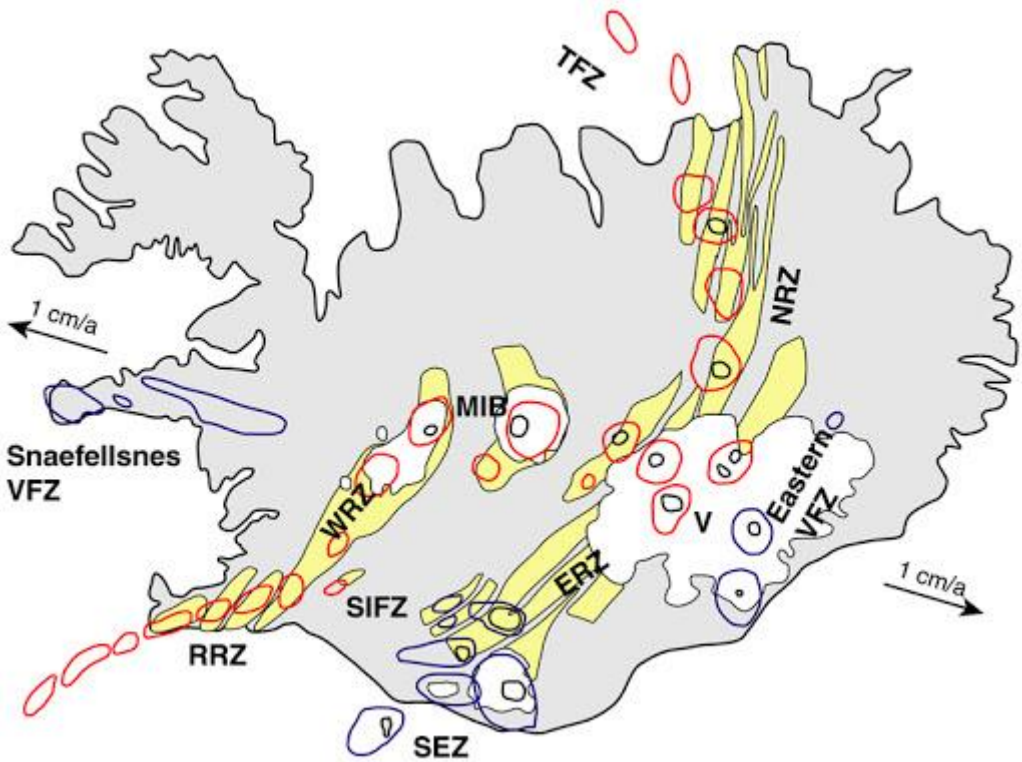

Figure 1. Distribution of volcanic systems within volcanic zones and belts in Iceland. Active volcanic systems are marked with red and inactive systems with blue. Volcanic zones and belts are marked with yellow. Abbreviations: VFZ: Volcanic Flank Zone; RRZ: Reykjanes Ridge Zone; WRZ: West Volcanic Zone; SIFZ: South Icelandic Fracture Zone; MIB: Mid-Iceland Belt; SEZ: South Eastern Zone; ERZ: Eastern Rift Zone; V: Vatnajökull; NRZ: Northern Rift Zone; TFZ: Tjörnes Fracture Zone (Trönnes, 2002).

2.2 The Bárðarbunga volcanic system

Bárðarbunga is one of the most active volcanic systems in Iceland. It has a total length of 190 km and an area of ~2500 km^2 (Figure 2). The volcanic system consists of a fissure swarm and a 60 km wide ice-capped central volcano located directly above the center of the Iceland magma plume (Thordarson & Höskuldsson, 2008). The area which now hosts Bárðarbunga was created as volcanic activity shifted to the south away from the NRZ and closer to the mantle plume approximately 2 million years ago (Jóhannesson, 1980). The tectonic structure of the Bárðarbunga volcanic system is complicated in that fissures differ in orientation in the fissure swarms extending from the central volcano. South of Vatnajökull towards Dyngjuháls the fissures have a SW-NE strike whereas north of the central volcano fissures have a N-S strike (Hjartardóttir, Einarsson, Magnúsdóttir, Björnsdóttir & Brandsdóttir, 2015).

Bárðarbunga has erupted 23 times in historical time, making it the second most active volcanic system in historic time after Grímsvötn. In terms of volume, Bárðarbunga has produced ~10 km^3 (DRE) of mainly basaltic lava and tephra which accounts for ~15% of erupted magma in Iceland in historical time (Thordarson & Larsen, 2007). The determining factor between pre-historic and historic lavas in Iceland is ~870 A.D. (Thordarson & Larsen,

2007). At the southwest end of the 190 km long Bárðarbunga fissure swarm lies the Torfajökull silicic complex (Figure 2). Prior studies have presented evidence suggesting that magma mixing occurs at the intersection of the Veiðivötn fissures and the Torfajökull silicic complex, both in the form of pre- and syn-eruptive magma mixing (e.g. Zellmer, Rubin, Grönvold & Jurado-Chichay, 2008; Mork, 1984).

This study focuses on the large historical lava Fjallsendahraun which was formed ~1362 A.D (Sigvaldason, 1992). It lies north of the Bárðarbunga central volcano, just south of Dyngjufjöll Ytri (Figure 3, a). The most recent Bárðarbunga lava, Holuhraun 2014-15 also lies north of Bárðarbunga whereas the other four lavas discussed in this study are south of the Bárðarbunga central volcano, three of them being historical (Tröllahraun 1862-64, Veiðivötn ~1477 and Vatnaöldur ~870 A.D). Tjörvahraun is a prehistoric lava (~150 A.D) south of Bárðarbunga (Table 1).

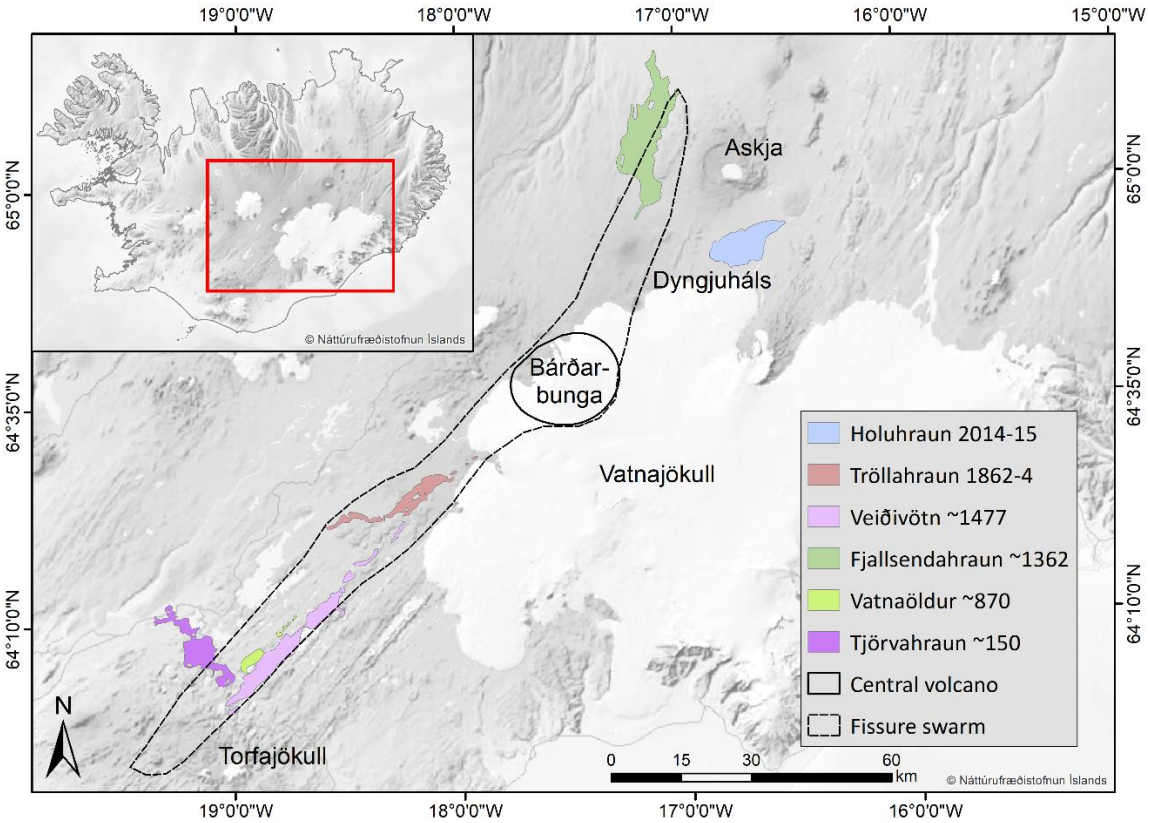

Figure 2. Simplified geological map of Bárðarbunga volcanic system in central Iceland. The Bárðarbunga volcanic system consists of a central volcano (solid outline) and a large fissure swarm (dashed outline). Lava units discussed in this paper are marked with colors. All units apart from Tjörvahraun are historic lavas, meaning younger than 1100 BP. Tjörvahraun is a prehistoric lava from 170 A.D. Map made by author based on geological map compiled by Haukur Jóhannesson published by the Icelandic Museum of Natural History and Iceland Geodetic Survey.

2.3 Recent fissure eruptions

Historic lavas from the Bárðarbunga volcanic system have been studied extensively. Jakobson (1979) studied and described the petrology of historical basalts from the ERZ, including lavas from Bárðarbunga. There he states that lavas from the southern part of the Bárðarbunga system (often referred to as the Bárðarbunga-Veiðivötn system) belong to the tholeiitic rock series and that geochemical variability in different lavas is mostly dependent on the amounts of macrophenocrysts (largely plagioclase). The eruptive history and styles of Tröllahraun, Veiðivötn and Vatnaöldur have been described by Thordarson and Larsen (2007). Þórarinsson and Sigvaldason (1972) used contemporary descriptions, chemical analysis and surface observations to study the formation of the Tröllahraun lava along with its craters.

Larsen (1984) described the volcanic history of the three major and most recent eruptions from the Veiðivötn fissure swarm: Tjörvahraun ~150 A.D, Vatnaöldur ~870 A.D and the ~1477 A.D Veiðivötn lava (Table 1). These three fissure eruptions are characterized as mainly basaltic, with minor amounts of silicic lava and tephra originating from fissures up to 42 km long. There is no evidence suggesting that other, smaller eruptions occurred during this period, suggesting that the Veiðivötn fissure swarm is inactive for long periods (600-800 years) between relatively large volcanic events (Larsen, 1984).

Name	**Year/s of eruption (A.D)**	**Duration**	**Volume - DRE (km^3)**	**Nr. of samples**
Holuhraun III	2014-15 *(1)*	6 months *(1)*	1,6 *(1)*	*11 *(a)*
Holuhraun II	1862-4 *(2)*	2 years *(2)*	-	*1 *(b)*
Tröllahraun	1862-4 *(3)*	2 years *(3)*	0,3 *(4)*	2
Veiðivötn	1477 *(3)*	69 hours *(5)*	1,1 *(5)*	1, *add. 2 *(c)*
Fjallsendahraun/ Frambruni	1362 *(6)*	-	4 *(3)*	11
Vatnaöldur	870 *(3)*	122 hours *(5)*	0,1 *(5)*	1
Tjörvahraun	150 *(5)*	200 hours *(5)*	0,8 *(5)*	1

*Table 1. List of lava units studied in this paper. The list states lava unit name, year/s of eruption, duration of eruption and unit volume. Note that Tröllahraun has a relatively small volume compared to eruption duration, this is because the eruption was characterized by intermittent effusive eruptions (Larsen and Guðmundsson, 2016). DRE: Dry Rock Equivalent. References: (1) Ilyinskaya, 2017 (2) Hartley & Thordarson, 2013 (3) Thordarson & Larsen, 2007 (4) Lasen & Guðmundsson, 2016 (5) Larsen, 1984 (6) Sigurgeirsson et al., 2015. Nr. of samples is the number of samples included in this study. *Additional samples used for comparison from: (a) Halldórsson et al., 2018 (b) Hartley and Thordarson (2013) (c) Caracciolo et al. (2020).*

The most thoroughly documented lava unit in Icelandic history is the 2014-15 Holuhraun eruption (Table 1). Note that in this study Holuhraun III and Holuhraun 2014-15 refers to the same lava unit. Holuhraun 2014-15 provided a rare opportunity to study magmatic processes and magma plumbing system dynamics during the 6-month basaltic fissure eruption (e.g. Bali et al., Hartley et al. Halldórsson 2018). Halldórsson et al. (2018) studied extensively the petrology and geochemistry of the eruption and concluded that the chemical composition of Holuhraun 2014-15 is nearly identical compared to other recent basaltic lavas from the Bárðarbunga volcanic system. They also discuss the magma reservoir body from which the eruption originates being relatively deep in the crust (8±5 km) and considerably primitive due to the lack in chemical variability which characterized eruptive products. On the basis of melt inclusions data, Hartley et al. (2018) demonstrated the likely occurrence of a calculated similar magma reservoir body depth (7.5 ± 2.5 km) for the 2014-15 Holuhraun lava from which the magma was transported laterally from underneath the Bárðarbunga central volcano to the eruption site further north.

2.4 The Fjallsendahraun lava

The ~1382 A.D Fjallsendahraun lava (Fjallsendi translates to mountain-end) is a result of a basaltic fissure eruption which occurred a few kilometers west of the Dyngjufjöll Ytri mountain complex which represents a subglacially-formed hyaloclastite ridge (Sigvaldason, 1992; Sigurgeirsson et al. 2015). The ridge is about 20 km long and 6 km wide with a maximum elevation of about 1000 m above sea level and an orientation of N25°E (Figure 3, a). Despite being volcanically extinct, volcanism still occurs adjacent to the Dyngjufjöll Ytri ridge. Sigvaldason (1992) describes recent hydrothermal explosion craters which he found on top of the Dyngjufjöll Ytri ridge. He suggests that these craters are related to a volcanic fissure originating from underneath the Dyngjufjöll Ytri hyaloclastite ridge, from which the Fjallsendahraun lava erupted. He further concludes that the formation of the crates was likely contemporaneous with the Fjallsendahraun eruption.

Despite its substantial volume (4 km^3) and area (Figure 2), the Fjallsendahraun lava has not been studied to an extent similar to other large historical fissure lavas from central Iceland. Sigmarsson and Halldórsson (2015) assigned the Fjallsendahraun lava to the Bárðarbunga volcanic system using Sr- and Nd-isotope ratios. Svavarsdóttir (2017) presented an extensive geochemical and radiogenic isotopic dataset where she included two samples from Fjallsendahraun. From analyzing whole rock composition, she concluded that the Fjallsendahraun lava originates from Dyngjuháls region and that it is one of the most evolved lava unit associated with the Bárðarbunga volcanic system. Note that Fjallsendahraun is also known as Frambruni but in this study the former will be used.

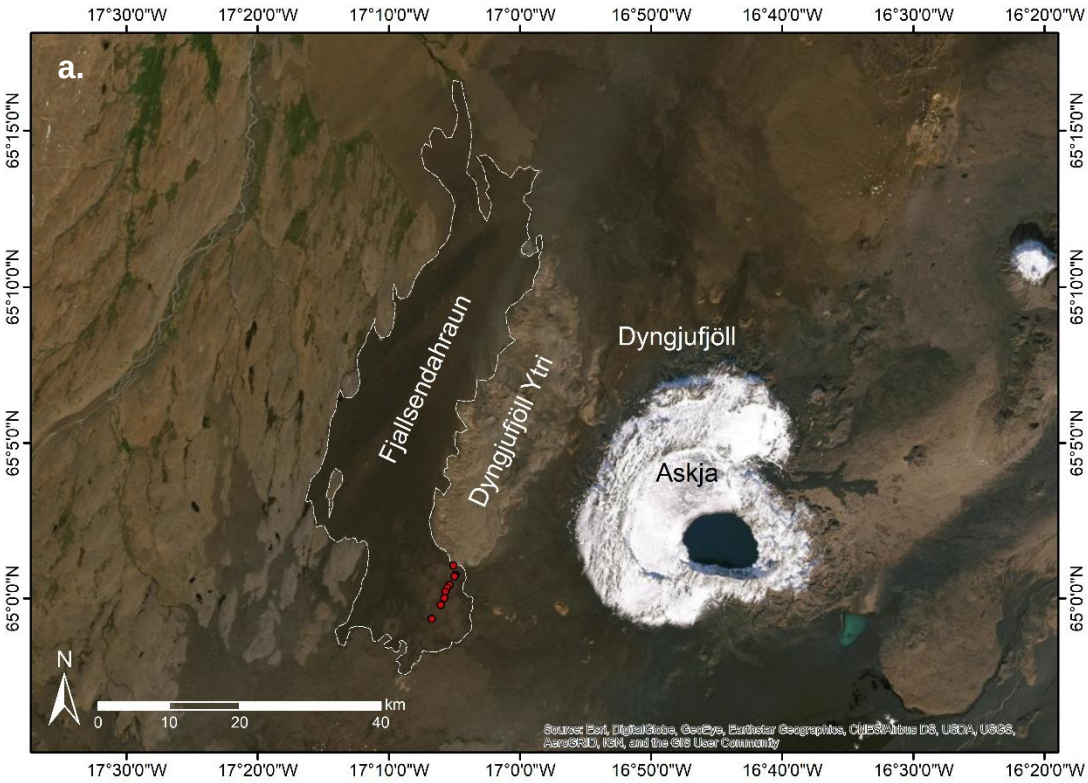
a.
17°30'0"W
17°20'0"W
17°10'0"W
17°0'0"W
16°50'0"W
16°40'0"W
16°30'0"W
16°20'0"W
65°15'0"N
65°10'0"N
65°5'0"N
65°0'0"N
Fjallsendahraun
Dyngjufjöll Ytri
Dyngjufjöll
Askja
N
km
0
10
20
40
Source: Esri, DigitalGlobe, GeoEye, Earthstar Geographics, CNES/Airbus DS, USDA, USGS, AeroGRID, IGN, and the GIS User Community

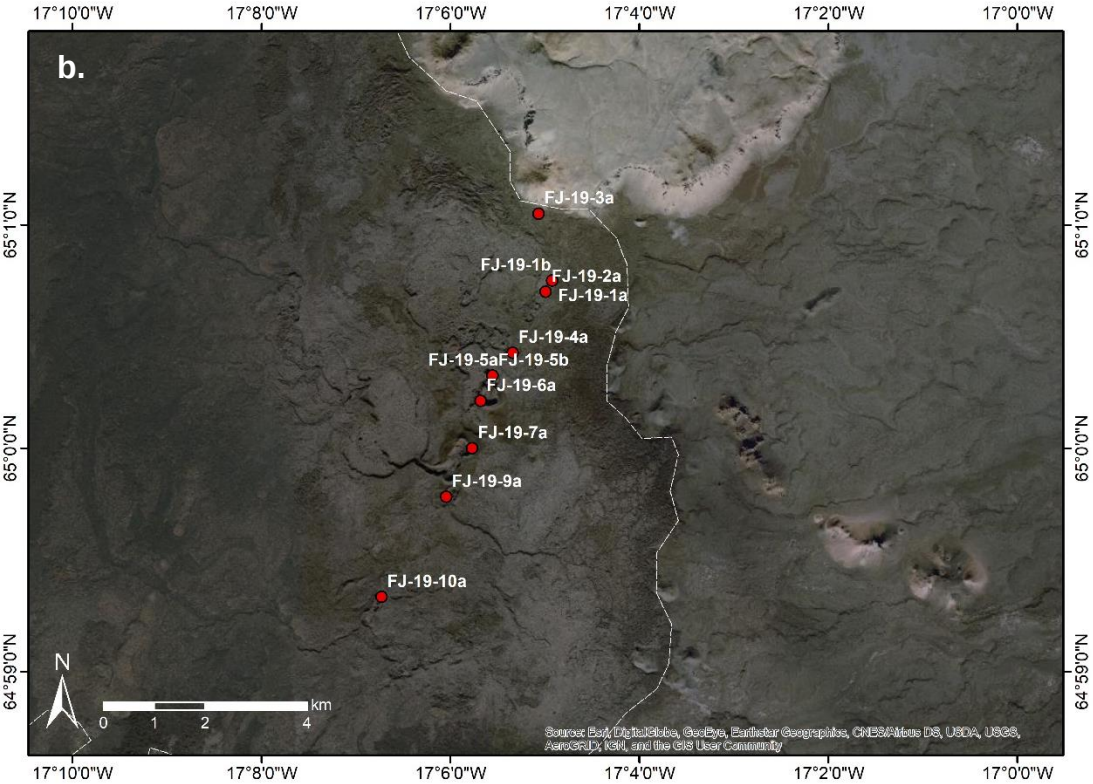

Figure 3. A: satellite imagery map of Fjallsendahraun and the surrounding area. Red dots represent sample locations. B: close up of sample locations on Fjallsendahraun with labels, all samples are taken from craters. Note that samples FJ-19-1a and 1b, as well as 5a and 5b, share the same GPS location point. Sources: Esri, DigitalGlobe, GeoEye, i-cubed, USDA FSA, USGS, AEX, Getmapping, Aerogrid, IGN, IGP, swisstopo, and the GIS User Community

3 Methods

3.1 Samples and sample preparation

A total of 16 samples were analyzed, including samples from Fjallsendahraun (11), Tröllahraun (2), Tjörvahraun (1), Vatnaöldur (1) and Veiðivötn (1) (Table 1). Sæmundur Ari Halldórsson and Edward Marshall collected the Fjallsendahraun samples in 2019 (Figure 3, b). Sæmundur, Karl Grönvold and Ken Rubin collected the Tröllahraun, Tjörvahraun, Vatnaöldur and Veiðivötn samples in 2008. Notably, all these samples were taken from the volcanic craters from which these lava units erupted with a particular focus given to fresh and glassy materials.

Sample preparation started with a preliminary sample inspection. All samples came in a one-liter bag, either as one large block or broken up into several hand sized pieces. The aim was to isolate glassy, clean looking tephra which is characterized by a dark color, glassy luster and absence of dirt and crystals. All samples had predominantly good quality glassy tephra. Hand sized tephra glass pieces from each sample were crushed using a hammer into grains varying in size from 1-3mm (Figure 4). Following this, 10-11 grains of fresh glassy scoria were hand-picked from each sample using a simple microscope and tweezers. The grains where placed on a small plate (~2 cm diameter) fitted with adhesive tape and then mounted in epoxy resin. Four epoxy mounts were prepared with ca. 40 grains per mount. The resin was then polished to expose the glass grains, starting with a fine sandpaper (120-220 grit) and moving up to diamond paste. The samples where then analyzed for major and minor elements using a JEOL JXA-8230 electron microprobe at the Institute of Earth Sciences, University of Iceland (Figure 4).

Additional sample EPMA data from Holuhraun 2014-15 was acquired from Halldórsson et al. (2018). Sample JS040914-07 from the Holuhraun 2014-15 data set is an outlier in terms of MgO and FeO weight%. This is because the glass was subject to in situ crystallization of microlites (Halldórsson et al., 2018) and so this sample is not included in the following data interpretations (Figures 13, 14). EPMA data from two additional Veiðivötn samples where acquired from Caracciolo et al. (2020). In addition, EPMA data from Holuhraun II was acquired from Hartley and Thordarson (2013) and finally tephra glass EPMA data from Bárðarbunga was acquired from Óladóttir, Larsen and Sigmarsson (2011) and used to create a representative liquid line of descent (lld) for Bárðarbunga magmas (Figure 9).

3.2 Analytical techniques and data evaluation

The electron probe micro-analyzer (EPMA) at the Institute of Earth Sciences, University of Iceland is a JEOL JXA-8230 SuperProbe equipped with a LaB6 thermionic electron emitter. It has five wavelength-dispersive spectrometers (WDS), one with four different analytical crystals and the other four WDS with two different crystals each. The accelerating voltage for the analyses was 15 keV, with a probe current of 10 nA, which was measured at the

Faraday cup prior to each analysis. To verify the analytical consistency and monitor instrumental drift of the electron microprobe, the international A99 standard was measured before and after sample analysis (Table 4, Appendix B). The A99 standard was provided courtesy of the Smithsonian Institution (NMNH standards) (Jarosewich, 2002).

Each glass grain was analyzed once with a beam diameter of 10 µm creating a data set with a total of 151 outputs. Sample EPMA data listing the chemical compositions of major and minor elements in weight% are listed in Table 5, Appendix C. The CITZAF correction program (Armstrong, 1991) was used for all analyses. Two glass grains from Fjallsendahraun (FJ-19-1a_4 and FJ-19-1a_7) are outliers in terms of compositional proportions. It is likely that these two points represent mineral compositions or areas affected by syn-eruptive crystallization. These sample grains (FJ-19-1a_4 and FJ-19-1a_7) are therefore excluded in data interpretation.

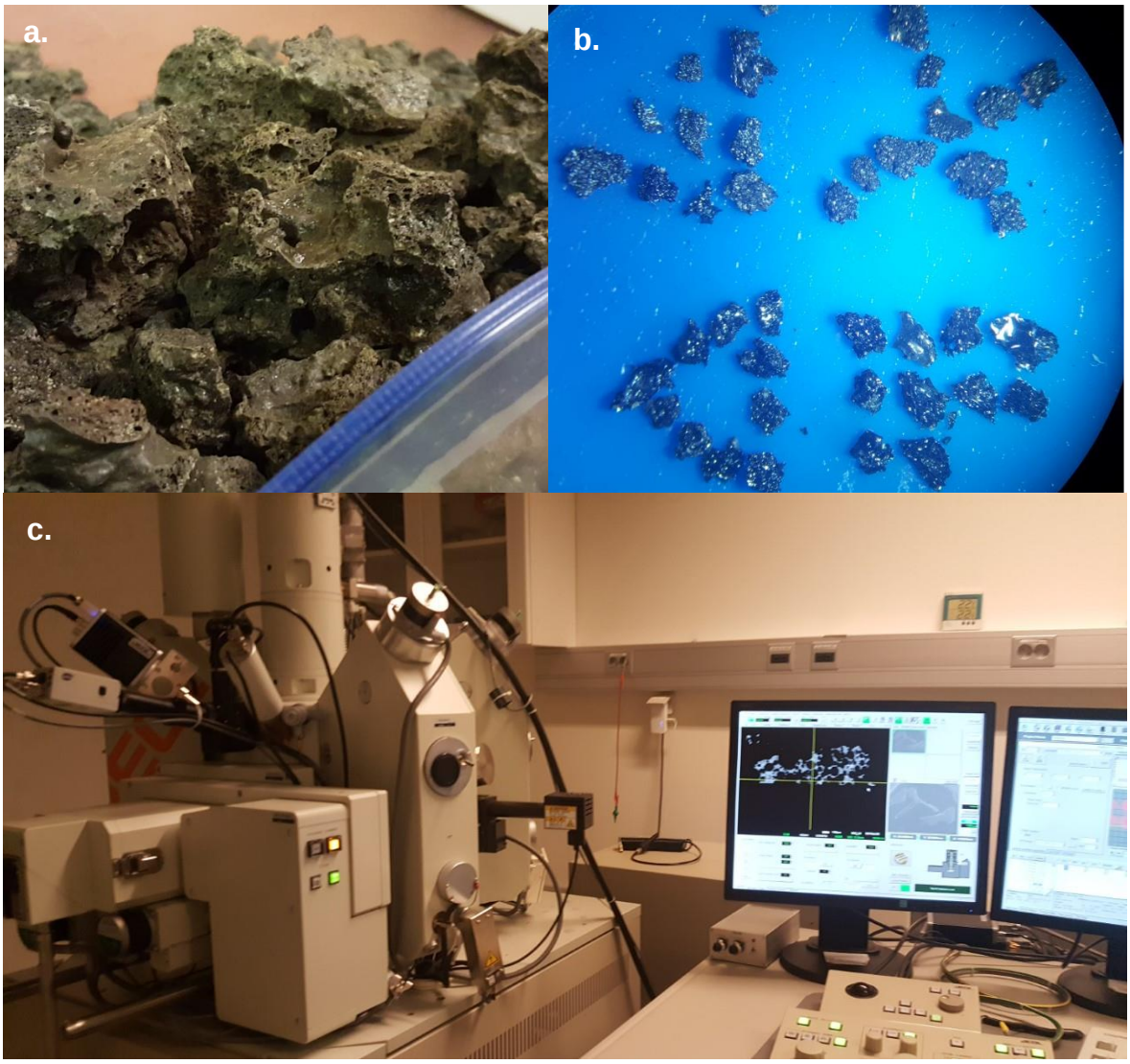

Figure 4. A: hand sized glassy tephra samples before being crushed B: hand-picked glassy tephra pieces from four localities mounted on a small plate (~2 cm in diameter) before being set in resin and polished. C: JEOL JXA-8230 electron microprobe at the Institute of Earth Sciences, University of Iceland.

4 Results

4.1 Petrography

Samples from Fjallsendahraun, Tjörvahraun, Tröllahraun, Veiðivötn and Vatnaöldur (Table 5) have similar textural and mineralogical features. In hand specimen, the tephra samples are vesicular with a glassy luster and macrocryst-poor (≤5 vol%; macrocrysts are defined here as minerals with long axes >1 mm). The BSE images captured by the microprobe (Figure 5, 6) reveal that the samples contain microphenocrysts (defined here as minerals with long axes between 100 µm and 1 mm) of mainly plagioclase and clinopyroxenes in a subophitic arrangement as is typical of Icelandic tholeiites (Jakobsson, 1979).

For comparison, Holuhraun tephra glass samples studied by Halldórsson et al. (2018) are also described as being macrocryst-poor and vesicular in hand specimen, with plagioclase and clinopyroxene microphenocrysts. Furthermore, Svavarsdóttir (2017) described whole rock samples from the Fjallsendahraun lava having a homogeneous, fine matrix with 5 vol% plagioclase and <2 vol% olivine macro- and microphenocrysts. Note that Svavarsdóttir's samples represent whole rock composition, whereas the samples in this study are tephra glass representing compositions which are likely closer to liquid melt compositions. In any case, this underlines the similarities in textural and mineralogical features in recent Bárðarbunga lavas.

The Fjallsendahraun sample grains (Figure 5) are dominated by silicate glass (≥95 vol%) with vesicles ranging in size from <100 µm to ∼1 mm. The grains contain elongated plagioclase microphenocrysts which appear dark grey in the BSE images and equant clinopyroxene microphenocrysts which appear light grey. The elongated plagioclase crystals in grain FJ-19-2a_5 (Figures 5, b) appear to have a similar orientation.

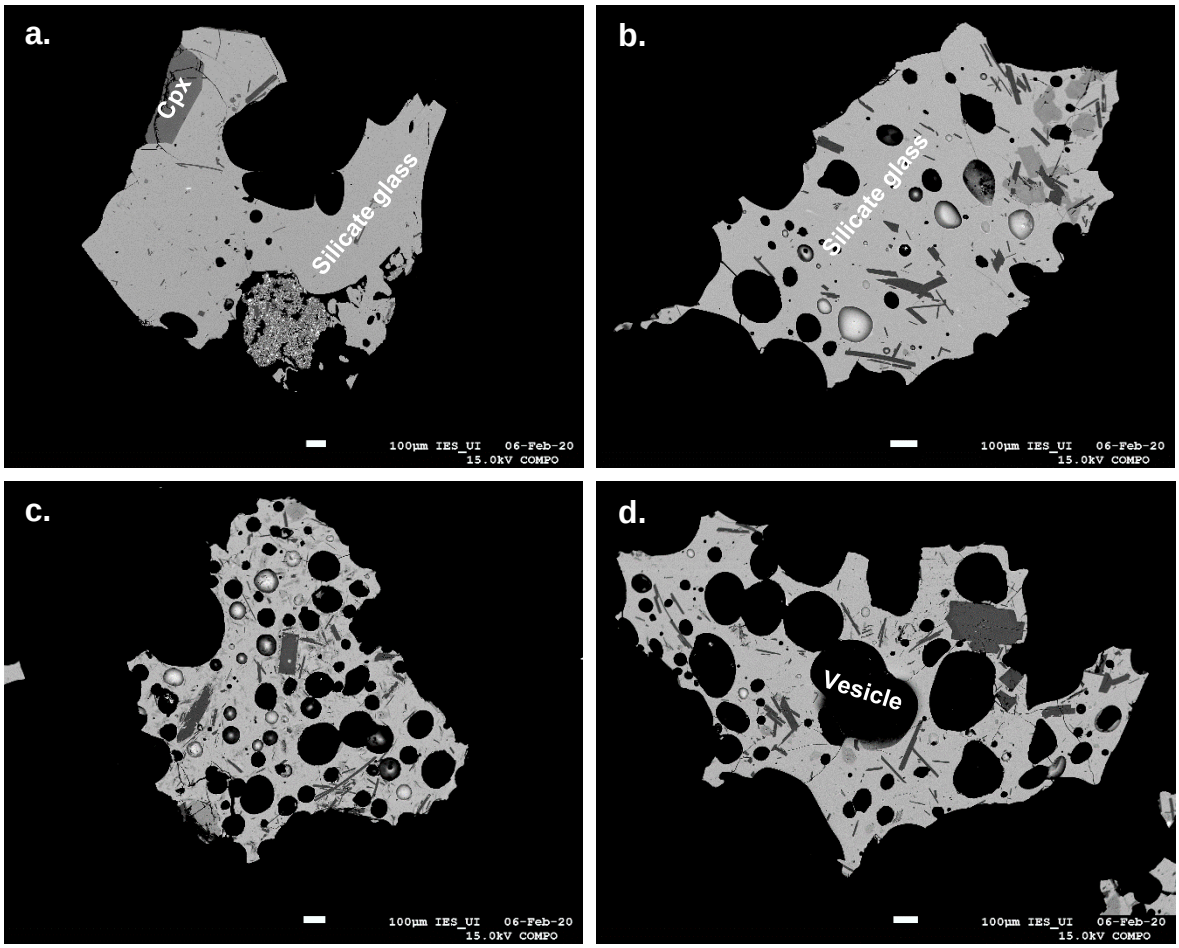

Figure 5. BSE images of Fjallsendahraun sample grains taken in the JEOL JXA-8230 electron microprobe. A: FJ-19-1a_4, note the large proportional volume of silicate glass (≥95 vol%) B: FJ-19-2a_5, note the common orientation of elongated plagioclase microphenocrysts. C: FJ-19-5b_10, D: FJ-19-10a_1, note the abundance of vesicles.

Tephra glass samples from the other four sample localities display similar mineralogical features as the Fjallsendahraun samples, especially Veiðivötn and Tröllahraun. The Veiðivötn sample grain (Figure 6, a) is slightly more enriched in plagioclase microphenocrysts which seem to have no common orientation and the Tröllahraun sample grain (Figure 6, c) is almost pure glass apart from a few (<10) plagioclase microphenocrysts. The Vatnaöldur sample grain (Figure 6, b) contains one large, fractured macrophenocryst (long axes >1 mm, ~50 vol%) with visible zonation whereas the Tjörvahraun sample grain (Figure 6, d) is dominated by vesicles with only a few visible crystals. The glass in the Tjörvahraun sample grain is slightly darker compared to other sample localities, indicating that the Tjörvahraun tephra glass composition is more enriched in heavier elements.

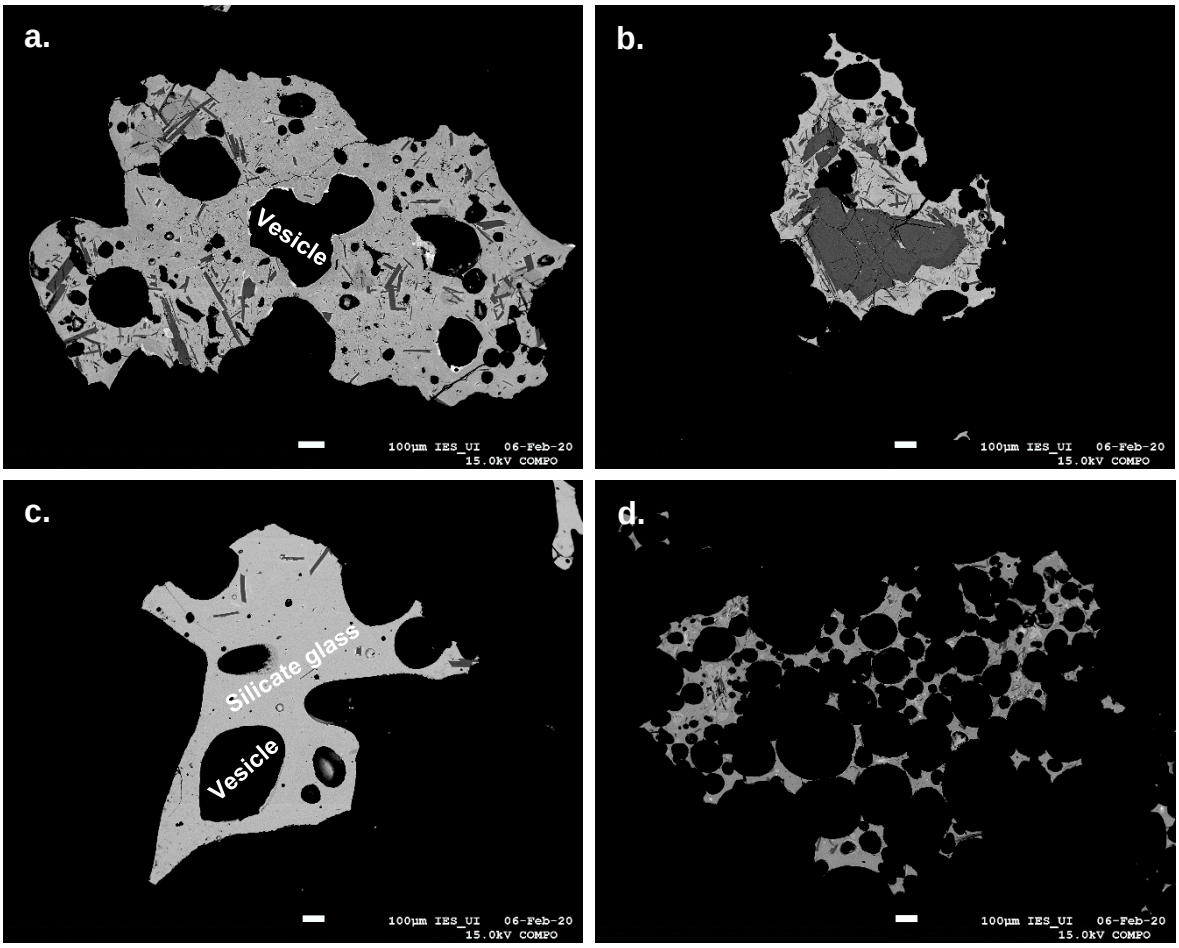

Figure 6. BSE images of sample grains taken in the JEOL JXA-8230 electron microprobe. A: Veiðivötn (V-2008-1a_3), note the increased volume of plagioclase microphenocrysts compared to other sample grains. B: Vatnaöldur (VO-2008-2_2), note the large, fractured macrophenocryst taking up ~50 % of the total grain volume. C: Tröllahraun (TR-2008-3b_1), note the large proportional volume of silicate glass (≥95 vol%). D: Tjörvahraun (TJ-2008-1_4), note the abundance of vesicles.

4.2 Glass composition

4.2.1 Classification

The compositional range of most major oxides of all sample spots analyzed is relatively small. All tephra glass samples apart from Tjörvahraun, are classified as basaltic on the Total Alkali Silica diagram (TAS, Figure 7), with silica content ranging from ~46-51 wt% and alkali content ranging from ~1,5-3 wt%. One sample spot from Fjallsendahraun (FJ-19-5b_1) is an outlier in terms of silica content (45,8 wt%). It is likely that this sample spot represents a silica-poor mineral composition instead of pure glass. The Tjörvahraun sample spots are more enriched in silica (~54-56 wt%) and alkali content (~3-6 wt%) and are therefore classified as basaltic andesite with one sample spot plotting as basaltic trachyandesite. One sample spot from Tjörvahraun (TJ-2008-1_8) is an outlier in terms of alkali content (2,9 wt%), likely reflecting a mineral composition or glass significantly

modified following emplacement. Both of these outlier spots (FJ-19-5b_1 and TJ-2008-1_8) will therefore be excluded in the remaining text. Thus, it is clear that Tjörvahraun has a substantially different composition compared to the other lava units which are near identical in silica and alkali content. This observation is in line with prior work suggesting that the Tjörvahraun magma was likely subject to chemical contamination by a rhyolitic melt originating from the Torfajökull silicic center which connects to the Bárðarbunga-Veiðivötn system in the south (Figure 2) (Larsen, 1984; Mork, 1984).

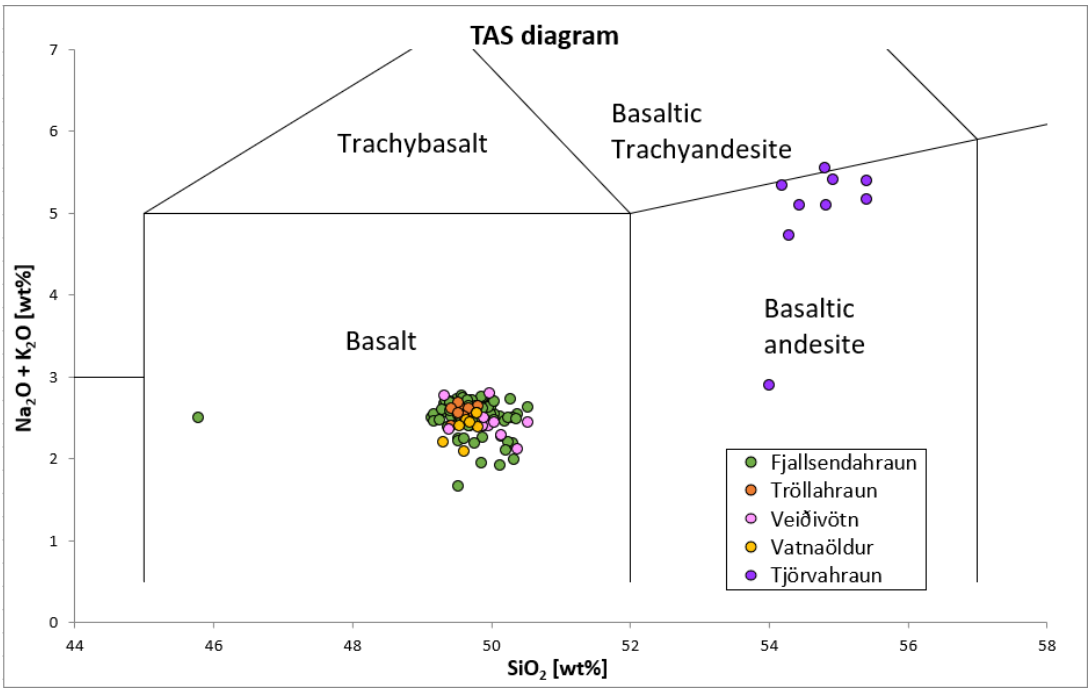

Figure 7. Total Alkali Silica (TAS) classification diagram with alkali content (Na_2O+K_2O) as a function of silica content (SiO_2). All components are in weight percent [wt%].

The AFM classification diagram (Figure 8) shows that the chemical affinity for all tephra glass sample spots studied in this work are tholeiitic. All sample spots except Tjörvahraun plot within or close to the tholeiitic magma series line, between basaltic and ferro-basaltic as is typical for Icelandic tholeiites (Jakobsson, 1979). The magma series line indicates the path of mafic magma evolution, starting at basaltic composition being less evolved and ending at rhyolite being more evolved. There is some correlation between sample locality and chemical affinity within the tholeiitic magma series, e.g. there is an increase in iron content between Tröllahraun, Vatnaöldur and Veiðivötn, respectively. Fjallsendahraun sample spots are more scattered with a majority of sample spots plotting close to the basaltic area of the tholeiitic magma series line, similar to Tröllahraun and Vatnaöldur. Note that there are 108 sample spots from Fjallsendahraun whereas there are around 10 sample spots for each of the other localities, causing the Fjallsendahraun sample spots to be more scattered.

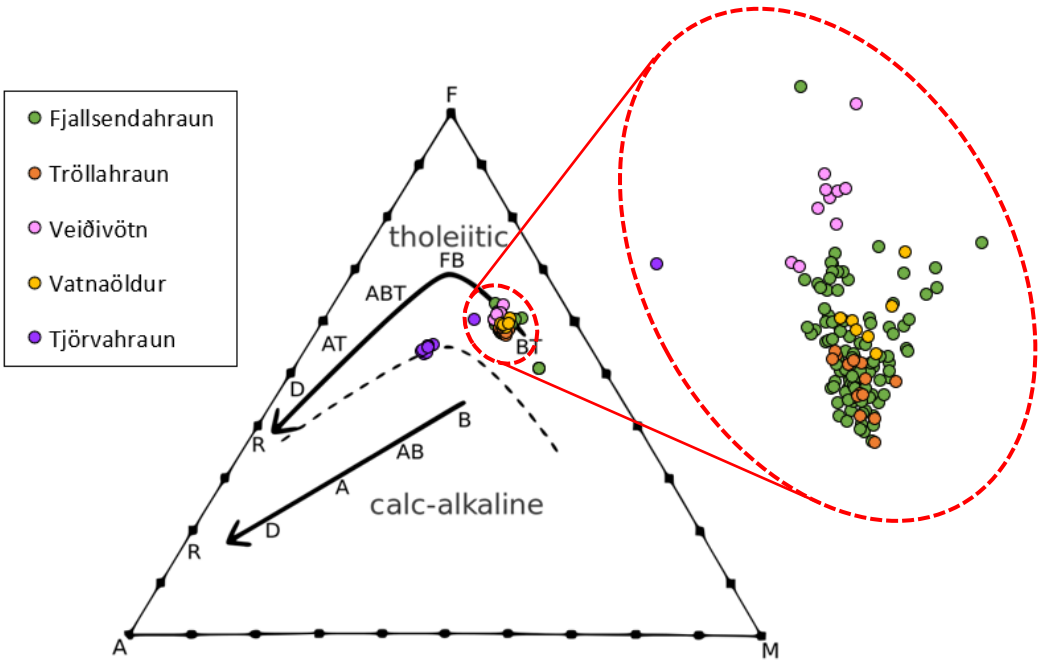

Figure 8. AFM classification diagram. A: Na_2O+K_2O, F: $FeO+Fe_2O_3$, M: MgO. The dotted line represents the partition between tholeiitic chemical affinity (above) and calc-alkaline affinity (below). The solid arrows represent the two corresponding magma series (tholeiitic and calc-alkaline) which show the path of mafic magma evolution. Abbreviations for the tholeiitic magma series (right to left): BT: basalt, FB: ferro-basalt, ABT: basaltic andesite, AT: andesite, D: dacite, R: rhyolite. All components are in weight percent [wt%].

4.2.2 Normative mineralogy

CIPW normative calculations were carried out using the Norm 4 software written by Kurt Hollocher of the Geology Department, Union College, New York State. These calculations reveal that of the 151 sample outputs, 121 are quartz normative and 30 are olivine normative (Figure 9) (Table 6, Appendix D). A majority of the quartz normative samples are from Fjallsendahraun (85 total) highlighting their evolved characteristics.

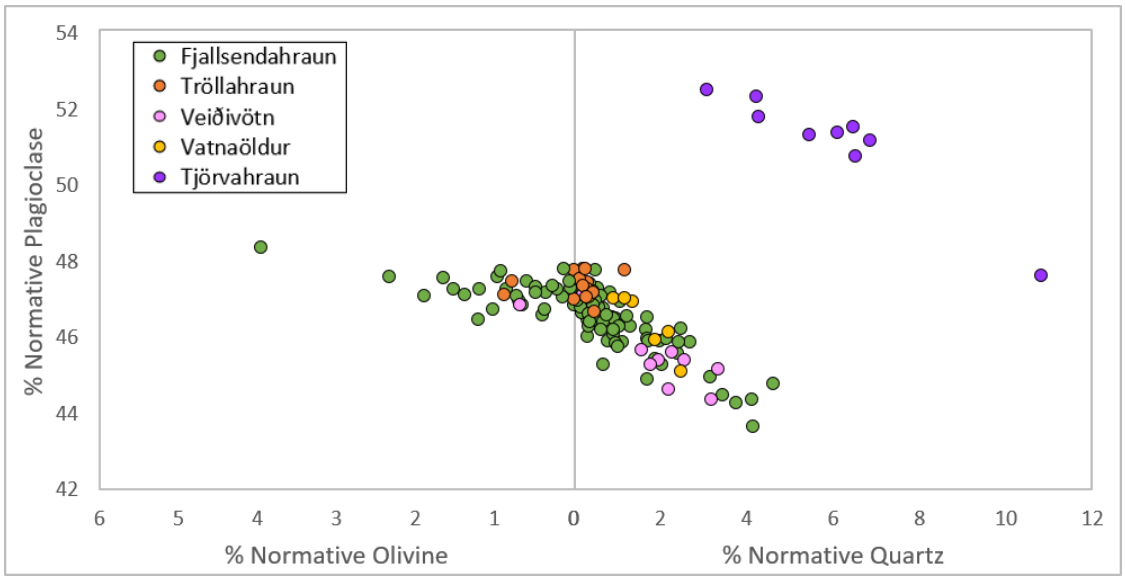

Figure 9. Plot of % normative plagioclase as a function of % normative olivine or quartz.

4.2.3 Internal variability

Internal variability within the Fjallsendahraun lava unit can be visualized with a Fenner diagram plotting TiO_2 as a function of MgO (Figure 10, a). MgO content ranges from ~6,1-6,9 wt%, with an average of 6,6 wt% whereas TiO_2 content ranges from ~1,60-1,95 wt% with an average of 1,82 wt%. There is a negative correlation between TiO_2 and MgO content. Besides one sample spot analyzed (FJ-19-5b_1), all the Fjallsendahraun glass spots reveal a very tight range of values.

Figure 10, b is also a Fenner diagram plotting TiO_2 as a function of MgO with the four other lava units included. Notably, Vatnaöldur and Tröllahraun samples are very similar to the Fjallsendahraun samples whereas the Veiðivötn sample is slightly more enriched in TiO_2 content (average is 1,98 wt%) and has a slight decrease in MgO content (average is 6,3 wt%). Veiðivötn, Vatnaöldur and Tröllahraun all seem to follow a common path of negative correlation whereas Tjörvahraun is substantially magnesium-poor compared to the other lava units with a MgO average of 4,1 wt%.

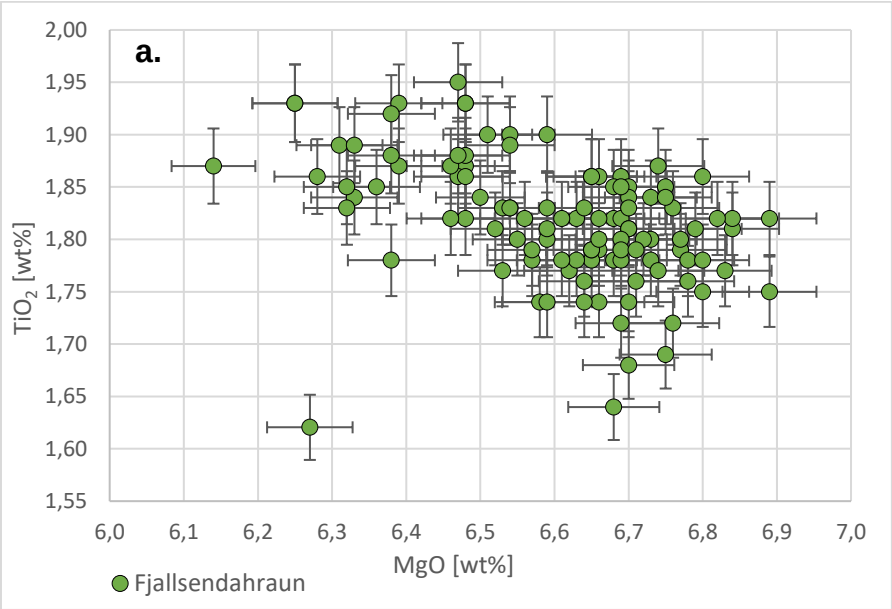

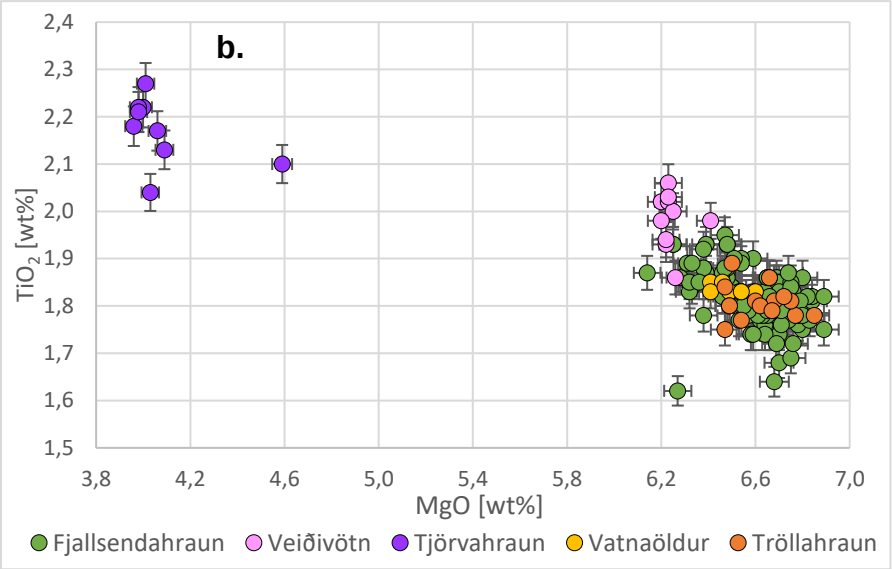

Figure 10. Two Fenner diagrams with TiO_2 as a function of MgO. A: Fjallsendahraun samples. B: All sample localities. Note the striking similarities of Fjallsendahraun and all samples besides Tjörvahraun.

4.3 Spatial variability

Samples from Fjallsendahraun where collected from craters at the northern part of the lava unit, starting at the lava front close to Dyngjufjöll and crossing over the lava field further north, creating a NE-SW oriented line (Figure 3, b). Figure 11 plots Fjallsendahraun samples with TiO_2 (Figure 11, a) and P_2O_5 (Figure 11, b) as a function of distance along the crater row, starting at 0 km at the northernmost crater (sample FJ-19-3a) and ending ~3,4 km further down south (sample FJ-19-10a).

The graphs show no obvious patterns that indicate any type of correlation between spatial distance and chemical composition. Concluded from the Fjallsendahraun tephra glass samples analyzed in this study, there is no spatial variability evident within the Fjallsendahraun lava unit.

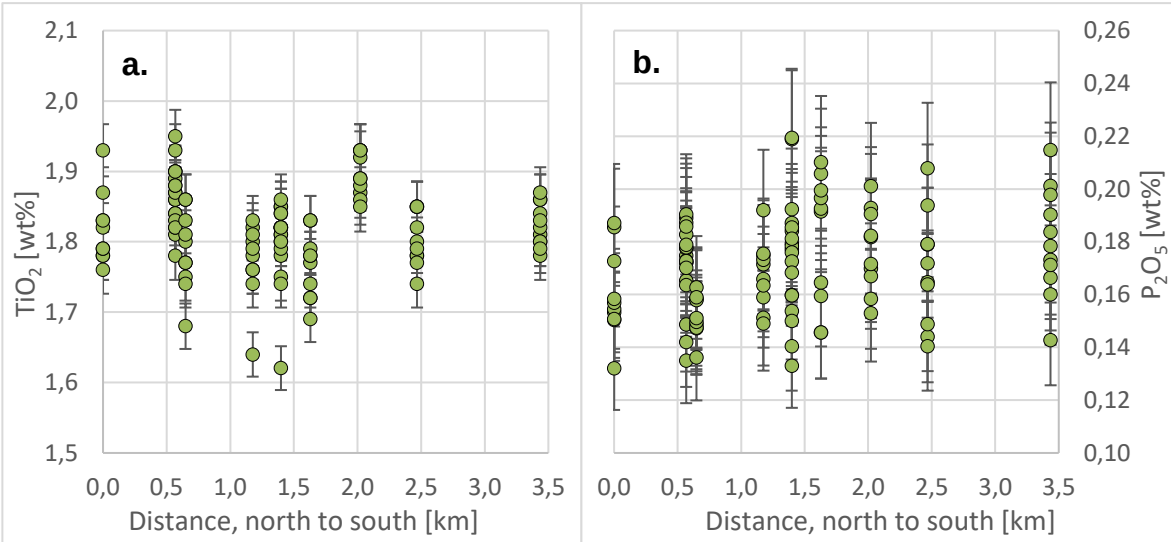

Figure 11. Two graphs plotting Fjallsendahraun samples with A. TiO_2 and B. P_2O_5 (weight percent [wt%]) as a function of distance after its craters. The distance goes from north to south, starting at the lava front close to Dyngjufjöll (sample FJ-19-3a) and moving ~3,4 km onto the center of the lava further south (sample FJ-19-10a).

A single sample from Veiðivötn was analyzed for this study (V-2008-1a) which originates from one of the northernmost volcanic craters of the Veiðivötn lava field. Two additional samples where acquired from Caracciolo et al. (2020), one from the southern part of the lava field and one from the center. Notably, all three samples come from volcanic craters of the Veiðivötn lava field.

Figure 12 plots the three Veiðivötn samples with TiO_2 (Figure 12, a) and P_2O_5 (Figure 12, b) as a function of distance along its craters, starting at 0 km at the southern part of the lava field and ending ~33,2 km further north. There is no visible correlation between spatial distance and chemical composition within the Veiðivötn lava unit.

The lack of spatial variability within the Fjallsendahraun and Veiðivötn lavas – even despite extensive length of volcanic fissure in case of the latter – concurs with observations from other fissures basalts from the Bárðarbunga volcanic system, e.g. the Holuhraun 2014-15 lava which also shows no evidence of spatial variability (Halldórsson et al., 2018).

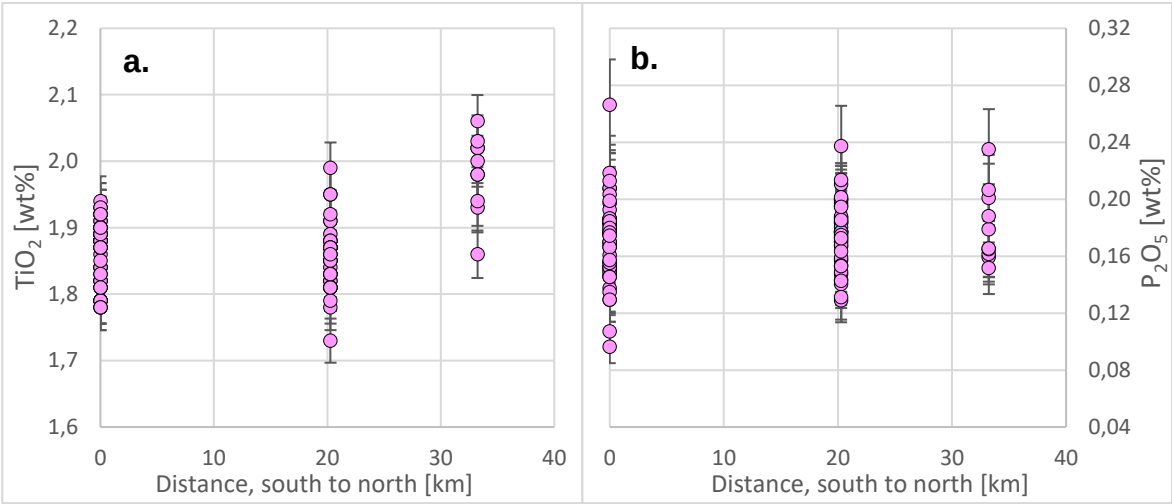

Figure 12. Two graphs plotting Veiðivötn samples with A. TiO_2 and B. P_2O_5 (weight percent [wt%]) as a function of distance along three of its craters. The samples from south and central Veiðivötn were acquired from Caracciolo et al. (2020).

5 Discussions

5.1 Fjallsendahraun and other recent fissure eruptions in the Bárðarbunga volcanic system: Chemical comparison

Figures 13 and 14 are diagrams plotting TiO_2 (Figure 13) and K_2O (Figure 14) as a function of MgO, included are the additional basaltic fissure lavas discussed above for comparison (Tjörvahraun not considered). In this case, the average of all analyzed sample grains from any given sample are plotted along with their corresponding percentage error.

The diagrams reveal that the chemical variability in glass composition between these six basaltic Bárðarbunga fissure lavas is relatively homogeneous. To add context the glass samples are compared to tephra samples from Bárðarbunga which span the last 3000+ years of Bárðarbunga volcanic activity and represent a likely liquid line of descent (lld) for Bárðarbunga magmas (Óladóttir et al., 2011). The glass samples studied here line up on the upper part of the lld (lower MgO and higher TiO_2 and K_2O), meaning they are more evolved. As magma evolves and is subject to fractional crystallization within a magma reservoir, MgO content in the liquid melt decreases whereas TiO_2 and K_2O content increases.

The youngest lava unit, Holuhraun 2014-15, is placed furthest up the lld, making it the most evolved (Figures 13, 14). Note that there are 11 samples from Holuhraun 2014-15 and only one sample from Holuhraun II and it plots within the Holuhraun 2014-15 sample area, slightly less evolved than the average for Holuhraun 2014-15. One sample from the center of the Veiðivötn lava is similarly evolved to the Holuhraun lavas, although with relatively low TiO_2 content compared to MgO content.

Fjallsendahraun is compositionally near identical to Vatnaöldur, Tröllahraun and the Veiðivötn north and south samples. Note that there are 11 samples from Fjallsendahraun and only 1-3 samples from other localities, so Fjallsendahraun samples take up a larger area. There is some difference between the least evolved samples, e.g. Tröllahraun is slightly less evolved than Veiðivötn.

There is some correlation between lava age and chemical composition. For example, two of the youngest lavas Holuhraun 2014-15 and Holuhraun II are slightly more evolved relative to older lavas. Tröllahraun and Holuhraun II are supposedly of similar age and yet they do not plot similarly. One explanation for this could be their location. Tröllahraun is situated on the southwest end of the Bárðarbunga fissure swarm and Holuhraun II in the northeast end (Figure 2). However, the difference in glass sample composition is on a relatively small scale with only ~1 wt% change in MgO content, highlighting the need to additional sampling of these two lava units.

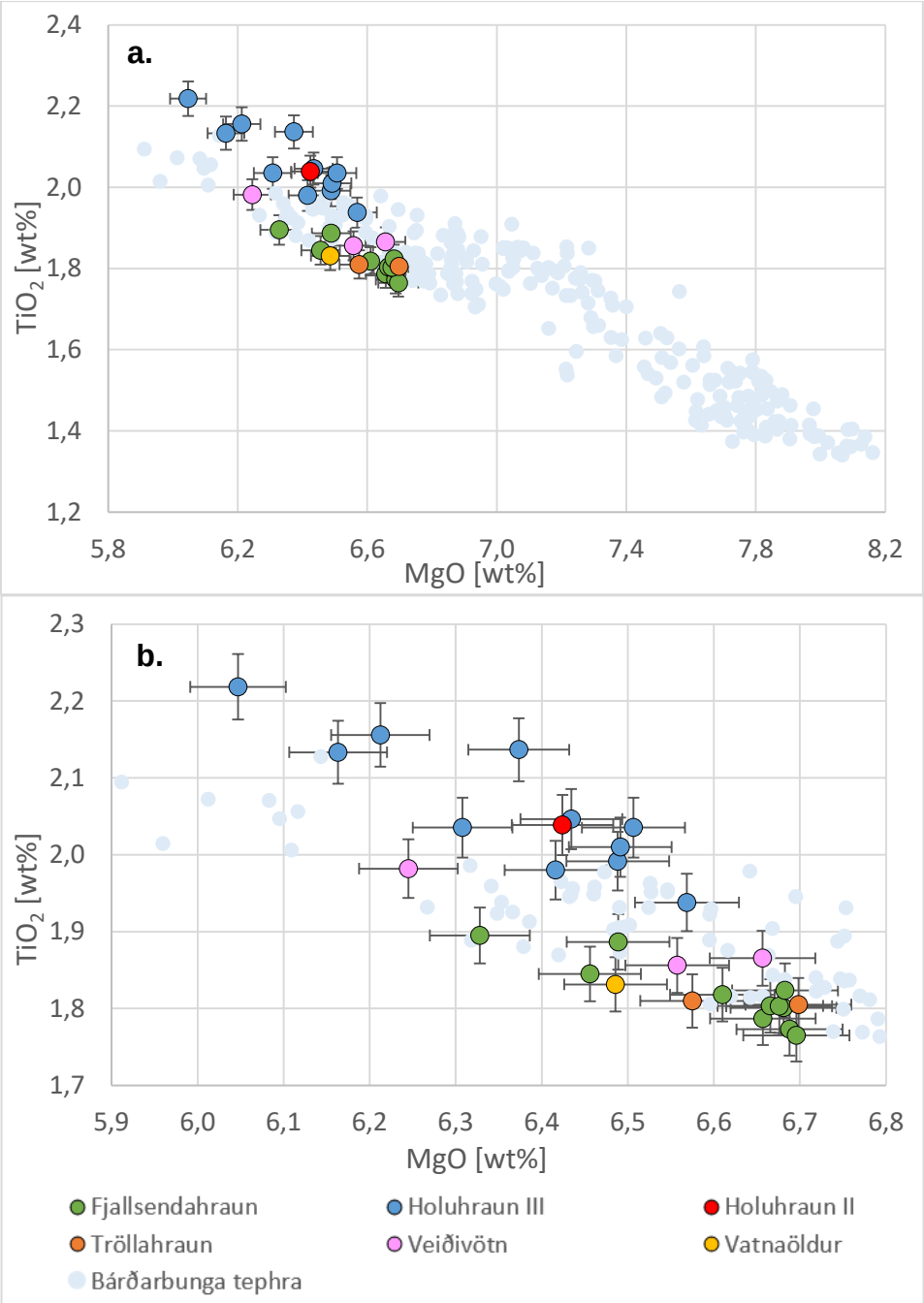

Figure 13. A: TiO_2 as a function of MgO B: same diagram on a narrower scale. Average oxide values are used for each sample, meaning that each point in the diagram represents a single sample. Bárðarbunga tephra (from Óladóttir et al., 2011) is an inferred liquid line of descent (lld) for Bárðarbunga magmas. All components are in weight percent [wt%].

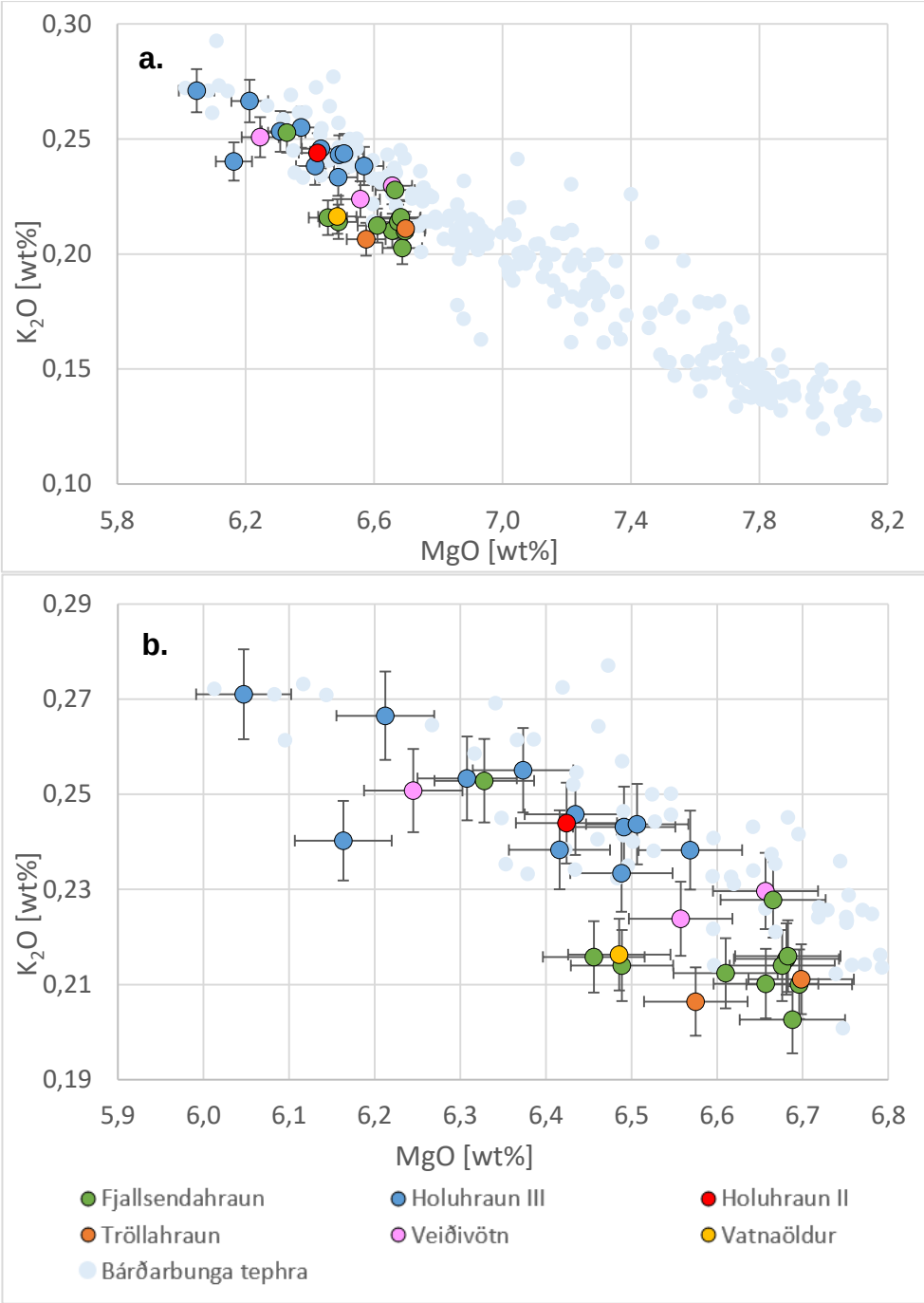

Figure 14. A: K_2O as a function of MgO B: same diagram on a narrower scale. Average oxide values are used for each sample, meaning that each point in the diagram represents a single sample. Bárðarbunga tephra represents a liquid line of descent (lld) for Bárðarbunga magmas. All components are in weight percent [wt%].

5.2 Thermobarometry: Constraining fractional crystallization depths

Having established that the studied lava units have near-identical chemical composition, the next step is to establish where they obtained their final composition within a shared magma body beneath the Bárðarbunga volcanic system. For this, pressures (or depth) of tephra glass equilibration was estimated using the position of the olivine–plagioclase–augite–melt (OPAM) thermal minimum as a barometer, given that the melt is saturated in all three mineral phases. Hartley, Bali, Maclennan, Neave and Halldórsson (2018) applied the implementation of the Yang et al. (1996) parameterization to create an improved version of the OPAM thermobarometer for Holuhraun 2014-15, the same approach is followed here. Only pressure outputs with a returned probability of $P_F < 0.8$ were used for further interpretation. (Tables 2, 7 - Appendix E). Included are the additional basaltic fissure lavas discussed above for comparison (Tjörvahraun not considered).

Name	**No. of outputs**	**P avg [kbar]**	**P range [kbar]**
Fjallsendahraun	28	1,85	0,94 - 2,60
Veiðivötn	11	1,60	1,09 - 2,40
Tröllahraun	1	1,89	-
Holuhraun II	4	1,57	1,08 - 2,35
Holuhraun III	121	2,08	0,46-3,38

Table 2: Results from OPAM thermobarometry calculations, following the same methods presented by Hartley et al. (2018). No. of outputs refers to the number of outputs that passed the $P_F < 0.8$ test. P avg refers to the average pressure for each sample locality. P range refers to the minimum and maximum pressure value for each sample locality. All OPAM calculation outputs are presented in Table 7 (Appendix E).

A majority of samples that passed the $P_F < 0.8$ test are from Holuhraun 2014-15 (Holuhraun III), which is to be expected as the thermobarometer was created for this lava unit specifically (Hartley et al., 2018). The average pressure for the 5 localities is similar, ranging from 1,57-2,08 kbar, which supports the idea of a shared mid-crustal magma body (Table 2). For reference, 2 kbar pressure is equal to ~6 km below sea level, which equals to ~8 km below Bárðarbunga (Sigmundsson et al., 2020). Figures 15 and 16 are diagrams plotting MgO (Figure 15) and TiO_2 (Figure 16) content as a function of pressure. Overall, the Holuhraun 2014-15 magma covers a large pressure range (~0,5-3,5 kbar) whereas Fjallsendahraun, Tröllahraun and Veiðivötn samples plot similarly with pressure ranging between ~1-2,5 kbar. None of the samples from Vatnaöldur passed the $P_F < 0.8$ test. Sample spots from sample JS040914 from Holuhraun 2014-15 have significantly low MgO, and high TiO_2 content compared to other samples, suggesting a more evolved composition.

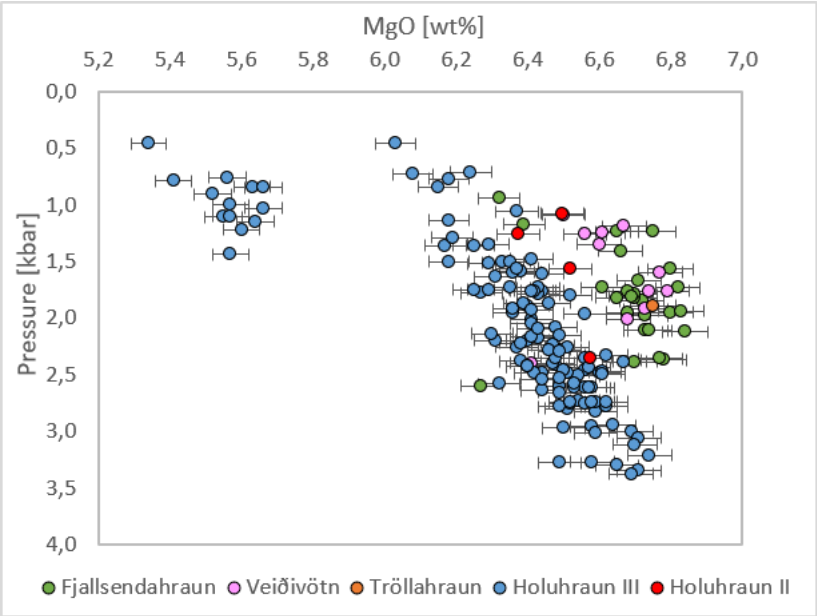

Figure 15. Pressure calculated using OPAM thermobarometry (Hartley et al., 2018) as a function of MgO content. Error bars for pressure values are ± 1,3 kbar.

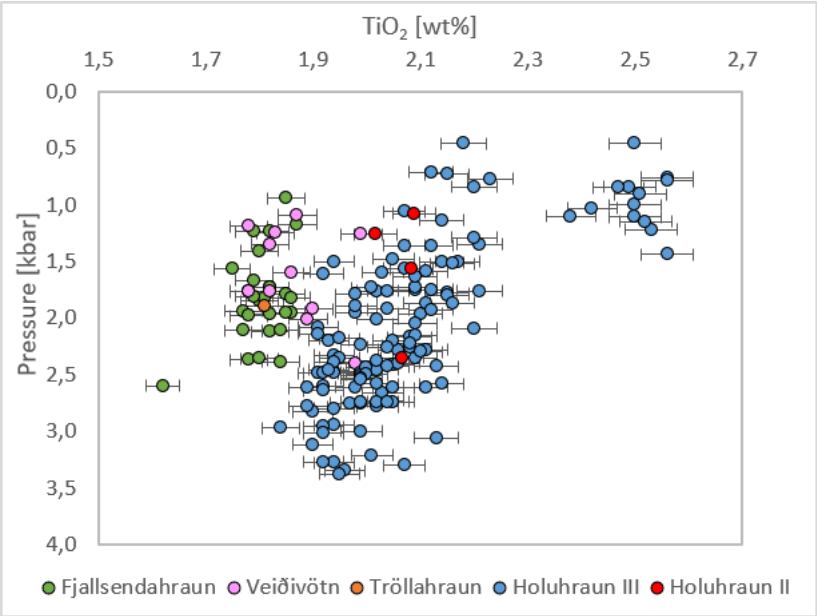

Figure 16. Pressure calculated using OPAM thermobarometry (Hartley et al., 2018) as a function of TiO_2 content. Error bars for pressure values are ± 1,3 kbar.

5.3 Implications for a common magma body beneath Bárðarbunga

Overall, the historical fissure lavas discussed are characterized by their lack of compositional variability and their alignment on the upper part of the inferred lld for Bárðarbunga magma (Figures 13, 14) (Óladóttir et al., 2011). Holuhraun 2014-15 is the most evolved of the lava units, followed by Holuhraun II (1862-64) and then older lavas which to some degree correlates to the year of eruption (Table 1). Furthermore, OPAM thermobarometry calculations support the idea that the discussed fissure lavas all originate from a similar depth in the middle of the crust (Figure 15, 16). Combined, these results support the idea of a common parental magma body which evolves with time and erupts as conditions in the crust are favorable.

As the Bárðarbunga magma body is filled, specific conditions within the crust related to rifting processes allows the magma to be transported by means of dykes and fissures. In the case of an eruption, magma is then moved laterally in the crust several tens of kilometers as was evident during the 2014-15 Holuhraun eruption (Halldórsson et al., 2018). This explains the lack of compositional variability between fissure lavas, despite them being situated at different ends of the 190 km long fissure swarm, apart from Tjörvahraun which must have been subject to magma mixing from the Torfajökull silicic complex (Mork, 1984). In recent times, the period between eruptions from the Bárðarbunga volcanic system appears to be limited to a few hundred years.

6 Conclusions

This study was focused on comparing compositional trends of Fjallsendahraun to recent basaltic fissure lavas from the Bárðarbunga volcanic system with a specific focus on the well-documented 2014-15 Holuhraun eruption. Major conclusions are:

- The ~1382 A.D Fjallsendahraun lava is composed of rather homogeneous olivine to quartz normative tholeiitic basalt.
- It's petrological characteristics and chemical compositions are near-identical to recent basaltic fissure lavas from the Bárðarbunga volcanic system.
- The basaltic part of Tjörvahraun is substantially different and reveals compositions more andesitic compared to the other Bárðarbunga lavas, suggesting magma mixing with Torfajökull magmas.
- Spatial variability within the Fjallsendahraun lava unit is very limited
- While the studied lava units cover a rather uniform compositional range, the most recent Bárðarbunga eruptive unit, Holuhraun 2014-15, reveals the most evolved compositions.
- A model supporting prior ideas of a single or common magma body beneath the Bárðarbunga volcanic system, being filled over time and erupting some few hundred years apart is favored.

References

Armstrong, J. T. (1991): Quantitative elemental analysis of individual microparticles with electron beam instruments. In: *Electron Probe Quantitation*. Springer US, Boston, MA, pp. 261–315. DOI: 10.1007/978-1-4899-2617-3_15.

Caracciolo, A., Bali, E., Guðfinnsson, G. H., Kahl, M., Halldórsson, S. A., Hartley, M. E. & Gunnarsson, H. (2020). Temporal evolution of magma and crystal mush storage conditions in the Bárðarbunga-Veiðivötn volcanic system, Iceland. *Lithos*. DOI: 10.1016/j.lithos.2019.105234

Einarsson, P. (2008). Plate boundaries, rifts and transforms in Iceland. *Jökull, 58*(35-58)

Halldórsson, S. A., Bali, E., Hartley, M. E., Neave, D. A., Peate, D. W., Guðfinnsson, G. H., … Thordarson, T. (2018). Petrology and geochemistry of the 2014–2015 Holuhraun eruption, central Iceland: compositional and mineralogical characteristics, temporal variability and magma storage. *Contributions to Mineralogy and Petrology, 173*(8). DOI: 10.1007/s00410-018-1487-9

Hartley, M. E., Bali, E., Maclennan, J., Neave, D. A., & Halldórsson, S. A. (2018). Melt inclusion constraints on petrogenesis of the 2014–2015 Holuhraun eruption, Iceland. *Contributions to Mineralogy and Petrology, 173*(2). DOI: 10.1007/s00410-017-1435-0

Hartley, M. E., & Thordarson, T. (2013). The 1874-1876 volcano-tectonic episode at Askja, North Iceland: Lateral flow revisited. *Geochemistry, Geophysics, Geosystems, 14*(7), 2286–2309. DOI: 10.1002/ggge.20151

Hjartardóttir, Á. R., Einarsson, P., Magnúsdóttir, E. S., Björnsdóttir, Þ. & Brandsdóttir B. (2015). Fracture Systems of the Northern Volcanic Rift Zone, Iceland: An Onshore Part of the Mid-Atlandic Plate Boundary. *Magmatic Rifting and Active Volcanism 420*, 297-314. DOI: 10.1144/sp420.1

Ilyinskaya, E., Schmidt, A., Mather, T. A., Pope, F. D., Witham, C., Baxter, P., … Edmonds, M. (2017). Understanding the environmental impacts of large fissure eruptions: Aerosol and gas emissions from the 2014–2015 Holuhraun eruption (Iceland). *Earth and Planetary Science Letters, 472*, 309–322. DOI: 10.1016/j.epsl.2017.05.025

Jakobsson, S. P. (1979). Petrology of recent basalts of the Eastern Volcanic Zone, Iceland. *Acta Naturalia Islandica, 26*, 1–103.

Jakobsson, S. P., Jónasson, K., Sigurðsson, I. A. (2008). The three igneous rock series of Iceland. *Jökull, 58*(177-138).

Jarosewich, E. (2002): Smithsonian Microbeam Standards. *J. Res. Natl. Inst. Stand. Technol. 107*, 681–685. DOI: 10.6028/jres.107.054

Jóhannesson, H. (1980). Jarðlagaskipan og þróun rekbelta á Vesturlandi. *Náttúrufræðingurinn 50*(1), 13-31.

Jóhannesson, H. & Sæmundsson, K. (1998). Geological map of Iceland, 1:500.000. Bedrock geology. Icelandic Institute of Natural History and Iceland Geodetic Survey, Reykjavík.

Larsen, G. (1984). Recent volcanic history of the Veidivötn fissure swarm, southern Iceland – an approach to volcanic risk assessment. *Journal of Volcanology and Geothermal Research, 22*(1-2), 33–58. DOI: 10.1016/0377-0273(84)90034-9

Larsen, G. & Guðmundsson, M.T. (2016). Bárðarbunga. In: Oladottir, B., Larsen, G. & Guðmundsson, M. T. Catalogue of Icelandic Volcanoes. IMO, UI and CPD-NCIP. Retrieved from http://icelandicvolcanoes.is/?volcano=BAR

Maclennan, J., Jull, M., McKenzie, D., Slater, L. & Grönvold, K. (2003). The link between volcanism and deglaciation in Iceland. *Geochemistry, Geophysics, Geosystems, 3*(11), 1-25. DOI: 10.1029/2001GC000282

Mork, M. E. (1984). Magma mixing in the post-glacial Veidivötn fissure eruption, southeast Iceland: a microprobe study of mineral and glass variations. *Lithos, 17*(55-75).

Óladóttir, B. A., Larsen, G. & Sigmarsson, O. (2011). Holocene volcanic activity at Grímsvötn, Bárdarbunga and Kverkfjöll subglacial centres beneath Vatnajökull, Iceland. *Bulletin of Volcanology, 73*(1187–1208). DOI: 10.1007/s00445-011-0461-4

Sigmarsson, O. & Halldórsson, S. A. (2015). Delimiting Bárðarbunga and Askja volcanic systems with Sr- and Nd-isotope ratios. *Jökull, 65*(17-27).

Sigmundsson, F., Pinel, V., Grapenthin, R., Hooper, A., Halldórsson, S. A., Einarsson, P., … Yamasaki, T. (2020). Unexpected large eruptions from buoyant magma bodies within viscoelastic crust. *Nature Communications, 11*(1). DOI: 10.1038/s41467-020-16054-6

Sigurgeirsson, M., Hjartarson, Á., Kaldal, I., Sæmundsson, K., Kristinsson, S.G. & Víkingsson S. (2015). *Jarðfræðikort af Norðurgosbelti. Syðri hluti – Ódáðahraun*. Reykjavík, Iceland Geosurvey 1.

Sigvaldason, G. E. (1992). Recent hydrothermal explosion craters in an old hyaloclastite flow, central Iceland. *Journal of Volcanology and Geothermal Research, 54*(1-2), 53–63. DOI: 10.1016/0377-0273(92)90114-s

Svavarsdóttir, S. I. (2017). *Geochemistry and petrology of Holocene lavas in the Bárðardalur region and their association with the Bárðarbunga volcanic system*. Master's thesis, Faculty of Earth Sciences, University of Iceland, pp. 130.

Thordarson, T. & Höskuldsson, Á. (2008). Postglacial volcanism in Iceland. *Jökull, 58*(197-228).

Thordarson, T. & Larsen, G. (2007). Volcanism in Iceland in historical time: Volcano types, eruption styles and eruptive history. *Journal of Geodynamics, 43*(118-152). DOI: 10.1016/j.jog.2006.09.005

Trönnes, R. G. (2002). Geology and geodynamics of Iceland. Nordic Volcanological Institute, University of Iceland, 1–19.

Yang, H.-J., Kinzler, R. J., & Grove, T. L. (1996). Experiments and models of anhydrous, basaltic olivine-plagioclase-augite saturated melts from 0.001 to 10 kbar. *Contributions to Mineralogy and Petrology*, *124*(1), 1–18. DOI: 10.1007/s004100050169

Zellmer, G. F., Rubin, K. H., Grönvold, K. & Jurado-Chichay, Z. (2008). On the recent bimodal magmatic processes and their rates in the Torfajökull-Veidivötn area, Iceland. *Earth and Planetary Science Letter 269*(388–398).

Þórarinsson, S. & Sigvaldason, G. E. (1972). Tröllagígar og Tröllahraun (The Tröllagígar eruption 1862–1864). *Jökull*, *22*(12-26).

Appendix A

Table 3: *Sample GPS points.*

Sample	Locality	LAT	LONG
FJ-19-1a	Fjallsendahraun	65,0125	-17,08203
FJ-19-1b	Fjallsendahraun	65,0125	-17,08205
FJ-19-2a	Fjallsendahraun	65,0117	-17,08319
FJ-19-3a	Fjallsendahraun	65,0175	-17,08446
FJ-19-4a	Fjallsendahraun	65,0071	-17,08902
FJ-19-5a	Fjallsendahraun	65,0054	-17,09259
FJ-19-5b	Fjallsendahraun	65,0054	-17,09258
FJ-19-6a	Fjallsendahraun	65,0035	-17,09468
FJ-19-7a	Fjallsendahraun	65,0000	-17,09618
FJ-19-9a	Fjallsendahraun	64,9964	-17,10073
FJ-19-10a	Fjallsendahraun	64,9889	-17,11214
Tj-2008-1	Tjörvahraun	64,3911	-19,2972
Tr-2008-2	Tröllahraun	64,2331	-18,1387
Tr-2008-3	Tröllahraun	64,2331	-18,1387
V-2008-1a	Veiðivötn	64,2231	-18,1491
VO-2008-2	Vatnaöldur	64,1351	-18,4036

Appendix B

Table 4: *Standard A99 EPMA data analyzed before and after sample analysis. A99 originates from the Smithsonian Institution in Washington DC, USA. All components are in weight percent [wt%]*

Sample	Point	SiO_2	TiO_2	Al_2O_3	FeO	MnO	MgO	CaO	Na_2O	K_2O	P_2O_5	Total
A99v	1	50,99	3,88	12,53	13,27	0,20	4,99	9,08	2,48	0,82	0,42	98,65
A99v	2	50,72	3,84	12,60	13,50	0,16	4,92	9,15	2,30	0,76	0,44	98,40
A99v	3	51,12	3,98	12,59	13,34	0,19	5,02	9,20	2,31	0,82	0,43	98,99
A99v	4	50,95	3,81	12,71	13,36	0,17	5,06	9,28	2,54	0,81	0,40	99,09
A99v	5	50,87	3,96	12,59	13,29	0,22	4,95	8,84	2,59	0,81	0,44	98,56
A99v	245	50,59	3,85	12,45	13,49	0,20	5,15	9,36	2,52	0,82	0,41	98,84
A99v	246	50,81	3,97	12,52	13,55	0,21	5,16	9,26	2,61	0,83	0,41	99,33
A99m	247	50,48	3,86	12,58	13,37	0,22	5,09	9,21	2,73	0,81	0,44	98,79
A99m	248	51,11	4,00	12,64	13,53	0,19	5,08	9,30	2,81	0,79	0,42	99,86
A99h	249	50,69	3,93	12,60	13,40	0,19	4,85	9,29	2,79	0,83	0,42	98,99
A99h	250	50,67	3,95	12,61	13,19	0,17	5,11	9,15	2,78	0,82	0,43	98,88
AVG		50,82	3,91	12,58	13,39	0,19	5,03	9,19	2,59	0,81	0,42	98,94
STD		0,200	0,062	0,064	0,111	0,019	0,094	0,136	0,172	0,018	0,014	0,380
Standard A99		50,94	4,06	12,49	13,49	0,15	5,08	9,30	2,66	0,82	0,38	99,39

Appendix C

Table 5*: *Sample EPMA data with average (AVG) and standard deviation (STD) for each sample. All components are in weight percent [wt%]

Sample	Locality	SiO_2	TiO_2	Al_2O_3	FeO	MnO	MgO	CaO	Na_2O	K_2O	P_2O_5	Total
FJ-19-1a_1	Fjallsendahraun	49,96	1,93	13,59	13,11	0,23	6,48	11,65	2,49	0,21	0,19	99,84
FJ-19-1a_2	Fjallsendahraun	49,67	1,84	13,69	13,18	0,22	6,33	11,56	2,36	0,22	0,17	99,24
FJ-19-1a_3	Fjallsendahraun	49,62	1,90	13,62	13,05	0,21	6,59	11,53	2,41	0,20	0,19	99,33
FJ-19-1a_4	Fjallsendahraun	49,02	1,14	14,81	10,36	0,17	8,09	13,48	1,89	0,09	0,07	99,12
FJ-19-1a_5	Fjallsendahraun	49,75	1,87	13,76	12,86	0,23	6,48	11,48	2,42	0,21	0,15	99,21
FJ-19-1a_6	Fjallsendahraun	50,01	1,90	13,69	13,02	0,23	6,54	11,58	2,34	0,21	0,14	99,65
FJ-19-1a_7	Fjallsendahraun	49,62	1,11	14,60	10,41	0,21	8,12	13,42	1,90	0,09	0,08	99,56
FJ-19-1a_8	Fjallsendahraun	49,84	1,95	13,53	13,26	0,21	6,47	11,63	2,44	0,21	0,17	99,71
FJ-19-1a_9	Fjallsendahraun	49,87	1,89	13,55	13,21	0,24	6,54	11,54	2,40	0,22	0,18	99,64
FJ-19-1a_10	Fjallsendahraun	49,33	1,86	13,54	13,35	0,24	6,47	11,56	2,45	0,22	0,17	99,19
FJ-19-1a_11	Fjallsendahraun	49,50	1,84	13,59	12,75	0,22	6,50	11,40	2,50	0,22	0,17	98,68
AVG	Fjallsendahraun	49,65	1,75	13,82	12,60	0,22	6,78	11,89	2,33	0,19	0,15	99,38
STD	Fjallsendahraun	0,291	0,310	0,448	1,107	0,017	0,657	0,773	0,219	0,051	0,042	0,337
FJ-19-1b_1	Fjallsendahraun	49,58	1,86	13,76	13,26	0,22	6,48	11,34	2,46	0,22	0,19	99,37
FJ-19-1b_2	Fjallsendahraun	49,89	1,87	13,68	13,05	0,22	6,46	11,62	2,46	0,21	0,14	99,61
FJ-19-1b_3	Fjallsendahraun	50,28	1,78	13,84	13,10	0,21	6,38	11,67	2,51	0,21	0,18	100,16
FJ-19-1b_4	Fjallsendahraun	49,70	1,88	13,58	13,03	0,22	6,48	11,57	2,37	0,21	0,17	99,21
FJ-19-1b_5	Fjallsendahraun	49,94	1,81	13,65	13,15	0,23	6,52	11,37	2,34	0,22	0,16	99,39
FJ-19-1b_6	Fjallsendahraun	49,85	1,82	13,44	13,06	0,23	6,48	11,50	2,44	0,21	0,17	99,21
FJ-19-1b_7	Fjallsendahraun	49,58	1,90	13,54	13,40	0,22	6,51	11,55	2,26	0,22	0,17	99,35
FJ-19-1b_8	Fjallsendahraun	49,91	1,88	13,61	13,17	0,25	6,47	11,57	2,41	0,22	0,18	99,66
FJ-19-1b_9	Fjallsendahraun	50,13	1,83	13,72	13,29	0,23	6,32	11,28	2,30	0,21	0,18	99,49
FJ-19-1b_10	Fjallsendahraun	50,38	1,82	13,77	13,32	0,23	6,46	11,71	2,33	0,22	0,19	100,43
AVG	Fjallsendahraun	49,92	1,85	13,66	13,18	0,23	6,46	11,52	2,39	0,22	0,17	99,59

Sample	Locality	SiO_2	TiO_2	Al_2O_3	FeO	MnO	MgO	CaO	Na_2O	K_2O	P_2O_5	Total
STD	Fjallsendahraun	0,273	0,038	0,120	0,128	0,010	0,061	0,144	0,081	0,005	0,013	0,405
FJ-19-2a_1	Fjallsendahraun	49,59	1,77	13,74	12,44	0,19	6,62	11,46	2,38	0,22	0,15	98,56
FJ-19-2a_2	Fjallsendahraun	49,75	1,86	13,79	12,69	0,22	6,80	11,50	2,44	0,21	0,16	99,43
FJ-19-2a_3	Fjallsendahraun	49,64	1,86	13,79	12,95	0,23	6,69	11,66	2,46	0,21	0,15	99,65
FJ-19-2a_4	Fjallsendahraun	50,03	1,75	13,70	12,75	0,21	6,80	11,60	2,47	0,21	0,15	99,66
FJ-19-2a_5	Fjallsendahraun	49,43	1,68	13,89	12,93	0,23	6,70	11,54	2,37	0,20	0,16	99,13
FJ-19-2a_6	Fjallsendahraun	49,78	1,83	13,86	12,85	0,19	6,59	11,49	2,41	0,21	0,16	99,37
FJ-19-2a_7	Fjallsendahraun	49,74	1,77	13,90	12,82	0,23	6,53	11,50	2,48	0,22	0,16	99,34
FJ-19-2a_8	Fjallsendahraun	49,87	1,80	13,87	12,67	0,23	6,59	11,56	2,33	0,20	0,15	99,28
FJ-19-2a_9	Fjallsendahraun	49,88	1,81	13,71	12,91	0,21	6,59	11,41	2,53	0,21	0,15	99,40
FJ-19-2a_10	Fjallsendahraun	49,70	1,74	13,75	13,05	0,19	6,66	11,55	2,37	0,21	0,14	99,36
AVG	Fjallsendahraun	49,74	1,79	13,80	12,81	0,21	6,66	11,53	2,42	0,21	0,15	99,32
STD	Fjallsendahraun	0,167	0,057	0,075	0,176	0,018	0,091	0,071	0,062	0,005	0,008	0,311
FJ-19-4a_1	Fjallsendahraun	49,87	1,80	13,84	12,83	0,23	6,73	11,76	2,42	0,20	0,15	99,84
FJ-19-4a_2	Fjallsendahraun	50,14	1,78	13,89	12,75	0,23	6,57	11,46	2,08	0,19	0,19	99,29
FJ-19-4a_3	Fjallsendahraun	50,31	1,79	13,96	12,70	0,22	6,77	11,58	2,30	0,20	0,17	100,01
FJ-19-4a_4	Fjallsendahraun	50,19	1,82	13,78	12,74	0,23	6,63	11,81	2,24	0,21	0,17	99,82
FJ-19-4a_5	Fjallsendahraun	49,61	1,81	13,90	12,79	0,23	6,84	11,74	2,38	0,20	0,17	99,66
FJ-19-4a_6	Fjallsendahraun	50,04	1,74	13,79	13,18	0,24	6,70	11,81	2,35	0,19	0,17	100,21
FJ-19-4a_7	Fjallsendahraun	49,83	1,64	13,90	12,65	0,24	6,68	11,72	2,32	0,19	0,16	99,33
FJ-19-4a_8	Fjallsendahraun	50,00	1,83	14,06	12,48	0,22	6,54	11,72	2,41	0,22	0,18	99,65
FJ-19-4a_9	Fjallsendahraun	49,99	1,76	13,92	12,85	0,24	6,64	11,61	2,33	0,21	0,16	99,71
FJ-19-4a_10	Fjallsendahraun	49,56	1,76	13,78	12,52	0,19	6,78	11,69	2,39	0,21	0,15	99,03
AVG	Fjallsendahraun	49,95	1,77	13,88	12,75	0,23	6,69	11,69	2,32	0,20	0,17	99,66
STD	Fjallsendahraun	0,229	0,052	0,084	0,185	0,015	0,090	0,105	0,096	0,009	0,012	0,337
FJ-19-7a_1	Fjallsendahraun	49,58	1,87	13,39	13,14	0,24	6,39	11,22	2,51	0,26	0,15	98,74
FJ-19-7a_2	Fjallsendahraun	50,53	1,86	13,65	13,22	0,23	6,28	11,39	2,36	0,26	0,17	99,95
FJ-19-7a_3	Fjallsendahraun	49,86	1,85	13,30	13,09	0,21	6,32	11,07	2,51	0,25	0,18	98,64

Sample	Locality	SiO_2	TiO_2	Al_2O_3	FeO	MnO	MgO	CaO	Na_2O	K_2O	P_2O_5	Total
FJ-19-7a_4	Fjallsendahraun	49,91	1,89	13,62	13,32	0,23	6,31	11,36	2,23	0,24	0,17	99,27
FJ-19-7a_5	Fjallsendahraun	50,05	1,93	13,47	13,27	0,21	6,39	11,42	2,22	0,25	0,19	99,40
FJ-19-7a_6	Fjallsendahraun	50,02	1,93	13,44	13,33	0,24	6,25	11,30	2,45	0,24	0,20	99,40
FJ-19-7a_7	Fjallsendahraun	50,24	1,92	13,66	13,30	0,24	6,38	11,23	2,24	0,26	0,18	99,65
FJ-19-7a_8	Fjallsendahraun	50,31	1,88	13,57	13,05	0,24	6,38	11,54	1,92	0,26	0,17	99,33
FJ-19-7a_9	Fjallsendahraun	49,96	1,89	13,61	13,26	0,21	6,33	11,19	2,38	0,24	0,16	99,23
FJ-19-7a_10	Fjallsendahraun	50,36	1,93	13,59	13,16	0,22	6,25	11,39	2,21	0,27	0,19	99,58
AVG	Fjallsendahraun	50,08	1,90	13,53	13,21	0,23	6,33	11,31	2,30	0,25	0,18	99,32
STD	Fjallsendahraun	0,280	0,031	0,123	0,099	0,012	0,056	0,136	0,179	0,010	0,016	0,392
FJ-19-5b_1	Fjallsendahraun	45,78	1,62	12,71	12,19	0,23	6,27	10,49	2,29	0,20	0,22	92,00
FJ-19-5b_2	Fjallsendahraun	49,14	1,75	14,04	12,93	0,21	6,89	11,42	2,29	0,21	0,14	99,02
FJ-19-5b_3	Fjallsendahraun	49,45	1,85	13,65	12,97	0,21	6,70	11,55	2,42	0,23	0,19	99,23
FJ-19-5b_4	Fjallsendahraun	49,50	1,82	13,62	12,86	0,20	6,68	11,32	2,35	0,21	0,18	98,74
FJ-19-5b_5	Fjallsendahraun	49,62	1,82	13,73	12,80	0,24	6,69	11,53	2,42	0,23	0,19	99,26
FJ-19-5b_6	Fjallsendahraun	49,61	1,85	13,78	12,92	0,21	6,68	11,45	2,46	0,23	0,18	99,36
FJ-19-5b_7	Fjallsendahraun	49,57	1,78	13,50	12,83	0,21	6,68	11,30	2,44	0,21	0,22	98,73
FJ-19-5b_8	Fjallsendahraun	49,71	1,82	13,70	13,13	0,19	6,84	11,57	2,50	0,21	0,18	99,85
FJ-19-5b_9	Fjallsendahraun	49,45	1,86	13,63	13,04	0,21	6,65	11,46	2,40	0,21	0,15	99,07
FJ-19-5b_10	Fjallsendahraun	49,77	1,84	13,72	13,07	0,22	6,73	11,39	2,41	0,22	0,15	99,52
AVG	Fjallsendahraun	49,16	1,80	13,61	12,87	0,21	6,68	11,35	2,40	0,22	0,18	98,48
STD	Fjallsendahraun	1,139	0,068	0,327	0,249	0,012	0,155	0,299	0,065	0,009	0,025	2,183
FJ-19-6a_1	Fjallsendahraun	49,77	1,74	13,74	13,05	0,22	6,64	11,42	2,37	0,21	0,19	99,35
FJ-19-6a_2	Fjallsendahraun	49,67	1,77	13,68	12,70	0,21	6,83	11,50	2,39	0,20	0,15	99,09
FJ-19-6a_3	Fjallsendahraun	49,86	1,78	13,61	12,80	0,21	6,69	11,54	1,73	0,22	0,19	98,63
FJ-19-6a_4	Fjallsendahraun	49,34	1,83	13,79	12,54	0,21	6,53	11,68	2,49	0,22	0,21	98,83
FJ-19-6a_5	Fjallsendahraun	49,17	1,72	13,82	12,86	0,24	6,69	11,38	2,33	0,21	0,20	98,61
FJ-19-6a_6	Fjallsendahraun	49,75	1,79	13,90	12,98	0,22	6,66	11,49	2,38	0,22	0,16	99,55
FJ-19-6a_7	Fjallsendahraun	49,90	1,83	13,68	12,76	0,22	6,76	11,84	2,19	0,21	0,21	99,61

Sample	Locality	SiO_2	TiO_2	Al_2O_3	FeO	MnO	MgO	CaO	Na_2O	K_2O	P_2O_5	Total
FJ-19-6a_8	Fjallsendahraun	50,25	1,78	13,92	12,78	0,23	6,65	11,51	2,00	0,20	0,16	99,49
FJ-19-6a_9	Fjallsendahraun	49,53	1,69	13,71	12,78	0,22	6,75	11,49	2,04	0,20	0,15	98,55
FJ-19-6a_10	Fjallsendahraun	49,38	1,72	13,59	12,86	0,23	6,76	11,52	2,18	0,20	0,20	98,64
AVG	Fjallsendahraun	49,66	1,77	13,74	12,81	0,22	6,70	11,54	2,21	0,21	0,18	99,04
STD	Fjallsendahraun	0,301	0,045	0,107	0,134	0,010	0,080	0,125	0,220	0,007	0,024	0,409
FJ-19-5a_1	Fjallsendahraun	49,59	1,82	13,67	12,80	0,23	6,61	11,33	2,50	0,24	0,18	98,96
FJ-19-5a_2	Fjallsendahraun	49,72	1,84	13,64	12,97	0,23	6,70	11,05	2,48	0,23	0,18	99,04
FJ-19-5a_3	Fjallsendahraun	49,61	1,80	13,76	12,98	0,20	6,72	11,60	2,41	0,24	0,19	99,51
FJ-19-5a_4	Fjallsendahraun	49,41	1,81	13,65	12,89	0,22	6,70	11,50	2,46	0,23	0,13	99,01
FJ-19-5a_5	Fjallsendahraun	49,81	1,81	13,71	12,97	0,23	6,70	11,62	2,37	0,23	0,16	99,61
FJ-19-5a_6	Fjallsendahraun	49,87	1,74	13,77	12,91	0,24	6,58	11,46	2,38	0,23	0,17	99,35
FJ-19-5a_7	Fjallsendahraun	49,73	1,79	13,63	12,81	0,24	6,65	11,42	2,40	0,21	0,18	99,06
FJ-19-5a_8	Fjallsendahraun	49,65	1,82	13,64	12,90	0,23	6,56	11,28	2,44	0,22	0,17	98,91
FJ-19-5a_9	Fjallsendahraun	49,34	1,80	13,70	12,82	0,23	6,77	11,33	2,34	0,22	0,16	98,71
AVG	Fjallsendahraun	49,64	1,80	13,69	12,89	0,23	6,67	11,40	2,42	0,23	0,17	99,13
STD	Fjallsendahraun	0,174	0,028	0,053	0,071	0,010	0,070	0,176	0,054	0,009	0,016	0,295
FJ-19-9a_1	Fjallsendahraun	49,73	1,78	13,74	13,13	0,20	6,63	11,64	2,20	0,22	0,14	99,41
FJ-19-9a_2	Fjallsendahraun	49,52	1,82	13,80	13,07	0,22	6,89	11,58	1,45	0,21	0,16	98,73
FJ-19-9a_3	Fjallsendahraun	49,48	1,78	13,64	13,27	0,25	6,73	11,64	2,23	0,22	0,16	99,41
FJ-19-9a_4	Fjallsendahraun	49,57	1,77	13,75	12,88	0,22	6,74	11,44	2,36	0,21	0,15	99,08
FJ-19-9a_5	Fjallsendahraun	49,43	1,80	13,61	12,86	0,22	6,69	11,59	2,31	0,20	0,17	98,89
FJ-19-9a_6	Fjallsendahraun	49,53	1,85	13,68	13,31	0,21	6,36	11,60	2,29	0,24	0,18	99,24
FJ-19-9a_7	Fjallsendahraun	49,45	1,85	13,64	13,14	0,20	6,69	11,59	2,38	0,24	0,21	99,38
FJ-19-9a_8	Fjallsendahraun	49,88	1,74	13,72	12,70	0,22	6,59	11,44	2,05	0,21	0,18	98,73
FJ-19-9a_9	Fjallsendahraun	50,05	1,85	13,56	13,23	0,26	6,75	11,82	2,50	0,20	0,19	100,41
FJ-19-9a_10	Fjallsendahraun	49,56	1,79	13,80	13,09	0,24	6,69	11,65	2,30	0,20	0,14	99,46
AVG	Fjallsendahraun	49,62	1,80	13,69	13,07	0,22	6,68	11,60	2,21	0,21	0,17	99,27
STD	Fjallsendahraun	0,204	0,038	0,081	0,197	0,022	0,137	0,108	0,291	0,014	0,022	0,491

Sample	Locality	SiO_2	TiO_2	Al_2O_3	FeO	MnO	MgO	CaO	Na_2O	K_2O	P_2O_5	Total
FJ-19-3a_1	Fjallsendahraun	49,29	1,93	13,77	13,55	0,25	6,48	11,25	2,37	0,23	0,19	99,31
FJ-19-3a_2	Fjallsendahraun	49,53	1,83	13,75	12,65	0,22	6,70	11,42	2,02	0,20	0,15	98,48
FJ-19-3a_3	Fjallsendahraun	49,18	1,78	13,64	12,76	0,21	6,61	11,76	2,26	0,20	0,15	98,55
FJ-19-3a_4	Fjallsendahraun	49,40	1,76	13,76	12,67	0,22	6,71	11,78	2,37	0,22	0,16	99,05
FJ-19-3a_5	Fjallsendahraun	49,78	1,78	13,84	12,80	0,22	6,78	11,30	2,44	0,20	0,13	99,27
FJ-19-3a_6	Fjallsendahraun	49,26	1,87	13,42	14,68	0,25	6,14	11,23	2,22	0,25	0,17	99,49
FJ-19-3a_7	Fjallsendahraun	49,66	1,79	13,62	12,65	0,23	6,65	11,58	2,49	0,22	0,15	99,03
FJ-19-3a_8	Fjallsendahraun	49,62	1,82	13,63	12,94	0,20	6,82	11,71	2,29	0,20	0,19	99,42
FJ-19-3a_9	Fjallsendahraun	49,58	1,83	14,01	12,63	0,21	6,64	11,74	2,37	0,20	0,15	99,37
FJ-19-3a_10	Fjallsendahraun	49,41	1,79	13,80	13,01	0,22	6,57	11,62	2,48	0,21	0,16	99,27
AVG	Fjallsendahraun	49,47	1,82	13,72	13,03	0,22	6,61	11,54	2,33	0,21	0,16	99,12
STD	Fjallsendahraun	0,194	0,051	0,158	0,642	0,016	0,192	0,220	0,141	0,018	0,017	0,352
FJ-19-10a_1	Fjallsendahraun	49,70	1,81	13,63	12,98	0,23	6,79	11,64	2,18	0,21	0,17	99,35
FJ-19-10a_2	Fjallsendahraun	49,73	1,78	13,85	13,08	0,23	6,80	11,35	2,23	0,22	0,14	99,42
FJ-19-10a_3	Fjallsendahraun	49,58	1,80	13,56	12,90	0,22	6,66	11,59	2,34	0,22	0,17	99,04
FJ-19-10a_4	Fjallsendahraun	49,61	1,86	13,51	13,06	0,25	6,66	11,81	2,02	0,23	0,20	99,21
FJ-19-10a_5	Fjallsendahraun	50,33	1,80	13,73	12,59	0,21	6,55	11,25	1,77	0,22	0,17	98,61
FJ-19-10a_6	Fjallsendahraun	49,58	1,82	13,66	12,83	0,24	6,66	11,83	2,24	0,21	0,18	99,25
FJ-19-10a_7	Fjallsendahraun	50,13	1,86	13,73	12,87	0,20	6,65	11,53	1,71	0,21	0,16	99,05
FJ-19-10a_8	Fjallsendahraun	49,68	1,84	13,58	12,79	0,22	6,75	11,80	2,18	0,21	0,19	99,25
FJ-19-10a_9	Fjallsendahraun	50,21	1,83	13,77	12,94	0,23	6,54	11,73	1,89	0,21	0,20	99,55
FJ-19-10a_10	Fjallsendahraun	49,76	1,87	13,73	12,94	0,24	6,74	11,75	1,98	0,21	0,21	99,43
FJ-19-10a_11	Fjallsendahraun	49,68	1,79	13,63	13,04	0,22	6,71	11,59	2,42	0,22	0,18	99,48
AVG	Fjallsendahraun	49,82	1,82	13,67	12,91	0,23	6,68	11,62	2,09	0,22	0,18	99,24
STD	Fjallsendahraun	0,271	0,031	0,101	0,141	0,013	0,086	0,190	0,231	0,007	0,020	0,265
V2008-1a_1	Veiðivötn	49,96	2,06	13,53	13,35	0,24	6,23	11,28	2,15	0,24	0,20	99,25
V2008-1a_2	Veiðivötn	49,87	2,02	13,63	13,57	0,24	6,20	11,25	2,15	0,25	0,21	99,39
V2008-1a_3	Veiðivötn	50,52	1,86	13,47	13,94	0,24	6,26	11,51	2,16	0,28	0,24	100,47

Sample	Locality	SiO_2	TiO_2	Al_2O_3	FeO	MnO	MgO	CaO	Na_2O	K_2O	P_2O_5	Total
V2008-1a_4	Veiðivötn	49,32	1,93	13,47	13,54	0,23	6,22	11,37	2,52	0,25	0,16	99,00
V2008-1a_5	Veiðivötn	49,39	2,02	13,53	13,59	0,24	6,23	11,29	2,10	0,25	0,16	98,80
V2008-1a_6	Veiðivötn	50,04	2,00	13,55	13,79	0,22	6,25	11,48	2,19	0,25	0,18	99,95
V2008-1a_7	Veiðivötn	49,97	1,98	13,66	13,84	0,25	6,41	10,88	2,56	0,23	0,16	99,95
V2008-1a_8	Veiðivötn	50,38	2,03	13,84	14,06	0,25	6,23	11,66	1,85	0,26	0,15	100,71
V2008-1a_9	Veiðivötn	50,15	1,94	13,58	13,51	0,22	6,22	11,00	2,04	0,25	0,17	99,07
V2008-1a_10	Veiðivötn	49,90	1,98	13,52	13,62	0,26	6,20	11,42	2,26	0,24	0,19	99,59
AVG	Veiðivötn	49,95	1,98	13,58	13,68	0,24	6,25	11,31	2,20	0,25	0,18	99,62
STD	Veiðivötn	0,377	0,059	0,111	0,219	0,012	0,061	0,234	0,211	0,012	0,026	0,640
TJ-2008-1_1	Tjörvahraun	55,40	2,22	15,47	10,81	0,22	4,00	5,78	3,55	1,84	0,30	99,59
TJ-2008-1_2	Tjörvahraun	54,81	2,22	15,23	11,21	0,17	3,98	6,02	3,84	1,71	0,30	99,49
TJ-2008-1_3	Tjörvahraun	54,29	2,27	14,93	10,74	0,17	4,01	7,19	3,32	1,40	0,31	98,63
TJ-2008-1_4	Tjörvahraun	55,41	2,17	15,48	11,32	0,20	4,06	5,80	3,50	1,67	0,34	99,95
TJ-2008-1_5	Tjörvahraun	54,19	2,13	15,19	10,96	0,21	4,09	7,18	3,80	1,53	0,34	99,62
TJ-2008-1_6	Tjörvahraun	54,82	2,18	15,32	11,04	0,20	3,96	5,79	3,39	1,70	0,35	98,75
TJ-2008-1_7	Tjörvahraun	54,92	2,21	15,44	11,14	0,18	3,98	5,80	3,55	1,86	0,32	99,40
TJ-2008-1_8	Tjörvahraun	54,00	2,10	15,31	11,27	0,20	4,59	8,92	2,01	0,88	0,33	99,61
TJ-2008-1_9	Tjörvahraun	54,43	2,04	15,11	11,08	0,19	4,03	7,20	3,62	1,48	0,29	99,47
AVG	Tjörvahraun	54,70	2,17	15,28	11,06	0,19	4,08	6,63	3,40	1,56	0,32	99,39
STD	Tjörvahraun	0,507	0,071	0,182	0,199	0,017	0,196	1,082	0,547	0,300	0,021	0,425
VO-2008-2_1	Vatnaöldur	49,65	1,85	13,93	12,85	0,20	6,41	11,71	2,25	0,22	0,11	99,18
VO-2008-2_2	Vatnaöldur	49,54	1,83	13,92	12,73	0,24	6,49	11,49	2,19	0,21	0,16	98,80
VO-2008-2_3	Vatnaöldur	49,61	1,83	13,84	13,19	0,24	6,60	11,63	1,85	0,24	0,18	99,21
VO-2008-2_4	Vatnaöldur	49,81	1,83	13,58	12,64	0,23	6,54	11,53	2,17	0,22	0,18	98,73
VO-2008-2_5	Vatnaöldur	49,79	1,85	13,90	13,09	0,21	6,46	11,79	2,35	0,21	0,15	99,80
VO-2008-2_6	Vatnaöldur	49,69	1,83	13,96	12,74	0,20	6,41	11,72	2,23	0,21	0,17	99,16
VO-2008-2_7	Vatnaöldur	49,31	1,80	13,83	12,71	0,21	6,49	11,53	1,99	0,21	0,18	98,26
AVG	Vatnaöldur	49,63	1,83	13,85	12,85	0,22	6,49	11,63	2,15	0,22	0,16	99,02

Sample	**Locality**	**SiO_2**	**TiO_2**	**Al_2O_3**	**FeO**	**MnO**	**MgO**	**CaO**	**Na_2O**	**K_2O**	**P_2O_5**	**Total**
STD	Vatnaöldur	0,170	0,017	0,129	0,210	0,017	0,069	0,115	0,170	0,009	0,026	0,483
TR-2008-3b_1	Tröllahraun	49,64	1,80	14,07	12,74	0,21	6,49	11,74	2,37	0,20	0,15	99,41
TR-2008-3b_2	Tröllahraun	49,67	1,81	13,91	12,62	0,24	6,60	10,93	2,36	0,20	0,15	98,49
TR-2008-3b_3	Tröllahraun	49,55	1,81	13,93	12,78	0,25	6,68	11,74	2,40	0,21	0,18	99,53
TR-2008-3b_4	Tröllahraun	49,81	1,84	13,82	12,88	0,21	6,47	11,64	2,45	0,19	0,20	99,51
TR-2008-3b_5	Tröllahraun	49,54	1,75	13,90	12,93	0,21	6,47	11,49	2,44	0,21	0,16	99,09
TR-2008-3b_6	Tröllahraun	49,70	1,78	13,84	13,00	0,23	6,77	11,59	2,36	0,21	0,18	99,66
TR-2008-3b_7	Tröllahraun	49,52	1,89	13,77	12,95	0,24	6,50	11,32	2,47	0,21	0,18	99,05
TR-2008-3b_8	Tröllahraun	49,61	1,80	13,94	12,87	0,19	6,62	11,65	2,32	0,21	0,16	99,36
AVG	Tröllahraun	49,63	1,81	13,90	12,85	0,22	6,58	11,51	2,40	0,21	0,17	99,26
STD	Tröllahraun	0,097	0,041	0,091	0,125	0,020	0,111	0,273	0,053	0,008	0,017	0,377
TR-2008-2_1	Tröllahraun	49,68	1,86	14,00	12,57	0,23	6,66	11,51	2,40	0,21	0,16	99,27
TR-2008-2_2	Tröllahraun	49,42	1,78	13,92	12,84	0,21	6,85	11,65	2,18	0,22	0,17	99,24
TR-2008-2_3	Tröllahraun	49,43	1,81	13,75	12,88	0,22	6,75	11,64	2,40	0,21	0,16	99,25
TR-2008-2_4	Tröllahraun	49,79	1,82	13,97	12,37	0,23	6,72	11,92	2,35	0,21	0,16	99,54
TR-2008-2_5	Tröllahraun	49,60	1,79	13,93	12,44	0,21	6,67	11,82	2,29	0,22	0,17	99,14
TR-2008-2_6	Tröllahraun	49,53	1,77	13,79	12,81	0,23	6,54	11,70	2,34	0,21	0,16	99,09
AVG	Tröllahraun	49,58	1,81	13,89	12,65	0,22	6,70	11,71	2,33	0,21	0,16	99,25
STD	Tröllahraun	0,145	0,033	0,101	0,221	0,010	0,103	0,145	0,083	0,006	0,005	0,156

Appendix D

Table 6**:** *CIPW normative calculations carried out using the Norm 4 software written by Kurt Hollocher of the Geology Department, Union College, New York State. All components are in percent [%].*

Sample	Locality	Quartz	Olivine	Plagioclase	Diopside	Anorthite	Albite	Hypersthene	Ilmenite	Magnetite	Orthoclase	Apatite	Total
FJ-19-1a_1	Fjallsendahraun	0,21	0,00	46,76	26,09	25,50	21,26	19,14	3,70	2,38	1,27	0,45	100
FJ-19-1a_2	Fjallsendahraun	0,68	0,00	46,78	25,28	26,51	20,27	19,58	3,55	2,41	1,31	0,42	100
FJ-19-1a_3	Fjallsendahraun	0,27	0,00	46,78	25,31	26,10	20,68	19,92	3,66	2,38	1,23	0,46	100
FJ-19-1a_4	Fjallsendahraun	0,00	3,95	48,37	28,74	32,14	16,23	14,16	2,20	1,89	0,51	0,17	100
FJ-19-1a_5	Fjallsendahraun	0,49	0,00	47,24	25,10	26,45	20,79	19,58	3,61	2,35	1,28	0,36	100
FJ-19-1a_6	Fjallsendahraun	0,90	0,00	46,53	25,33	26,52	20,01	19,65	3,65	2,37	1,25	0,32	100
FJ-19-1a_7	Fjallsendahraun	0,00	2,32	47,60	28,88	31,36	16,24	16,45	2,13	1,89	0,54	0,18	100
FJ-19-1a_8	Fjallsendahraun	0,33	0,00	46,46	26,08	25,61	20,86	19,31	3,74	2,41	1,25	0,41	100
FJ-19-1a_9	Fjallsendahraun	0,50	0,00	46,38	25,48	25,84	20,53	19,88	3,63	2,41	1,29	0,44	100
FJ-19-1a_10	Fjallsendahraun	0,00	1,01	46,74	26,00	25,68	21,06	18,47	3,59	2,44	1,34	0,41	100
FJ-19-1a_11	Fjallsendahraun	0,06	0,00	47,32	25,50	25,73	21,59	19,48	3,57	2,34	1,32	0,40	100
FJ-19-1b_1	Fjallsendahraun	0,04	0,00	47,31	24,47	26,21	21,10	20,41	3,58	2,42	1,32	0,45	100
FJ-19-1b_2	Fjallsendahraun	0,23	0,00	47,00	25,96	25,95	21,05	19,23	3,59	2,38	1,26	0,34	100
FJ-19-1b_3	Fjallsendahraun	0,31	0,00	47,37	25,68	26,02	21,36	19,18	3,40	2,37	1,26	0,42	100
FJ-19-1b_4	Fjallsendahraun	0,64	0,00	46,55	25,58	26,19	20,36	19,55	3,63	2,38	1,27	0,41	100
FJ-19-1b_5	Fjallsendahraun	0,96	0,00	46,51	24,51	26,44	20,07	20,43	3,48	2,40	1,32	0,39	100
FJ-19-1b_6	Fjallsendahraun	0,52	0,00	46,43	25,89	25,47	20,96	19,56	3,51	2,39	1,29	0,42	100
FJ-19-1b_7	Fjallsendahraun	0,79	0,00	45,91	25,20	26,51	19,39	20,25	3,66	2,45	1,33	0,41	100
FJ-19-1b_8	Fjallsendahraun	0,51	0,00	46,55	25,55	25,94	20,61	19,64	3,61	2,40	1,32	0,43	100
FJ-19-1b_9	Fjallsendahraun	1,69	0,00	46,54	23,72	26,84	19,71	20,43	3,52	2,42	1,24	0,43	100
FJ-19-1b_10	Fjallsendahraun	1,03	0,00	46,33	25,24	26,55	19,78	19,80	3,47	2,41	1,29	0,44	100
FJ-19-2a_1	Fjallsendahraun	0,56	0,00	47,32	25,04	26,74	20,58	19,70	3,43	2,29	1,30	0,36	100
FJ-19-2a_2	Fjallsendahraun	0,00	0,03	47,29	25,00	26,38	20,91	20,11	3,58	2,32	1,28	0,39	100

FJ-19-2a_3	Fjallsendahraun	0,00	1,18	47,27	25,80	26,23	21,04	18,18	3,57	2,36	1,28	0,36	100
FJ-19-2a_4	Fjallsendahraun	0,00	0,13	47,06	25,76	25,94	21,12	19,76	3,36	2,32	1,26	0,35	100
FJ-19-2a_5	Fjallsendahraun	0,00	0,59	47,47	24,80	27,09	20,38	19,94	3,24	2,37	1,22	0,38	100
FJ-19-2a_6	Fjallsendahraun	0,36	0,00	47,41	24,76	26,74	20,67	19,96	3,52	2,35	1,25	0,38	100
FJ-19-2a_7	Fjallsendahraun	0,00	0,12	47,79	25,00	26,52	21,28	19,66	3,41	2,34	1,29	0,38	100
FJ-19-2a_8	Fjallsendahraun	0,83	0,00	47,18	24,77	27,18	20,00	19,87	3,47	2,32	1,21	0,36	100
FJ-19-2a_9	Fjallsendahraun	0,00	0,05	47,47	25,25	25,78	21,69	19,78	3,48	2,36	1,24	0,36	100
FJ-19-2a_10	Fjallsendahraun	0,13	0,00	46,95	25,25	26,62	20,33	20,34	3,35	2,38	1,27	0,33	100
FJ-19-4a_1	Fjallsendahraun	0,00	0,35	47,19	25,85	26,53	20,66	19,26	3,45	2,33	1,21	0,36	100
FJ-19-4a_2	Fjallsendahraun	2,49	0,00	46,25	23,12	28,40	17,85	20,77	3,43	2,33	1,15	0,46	100
FJ-19-4a_3	Fjallsendahraun	1,08	0,00	46,95	24,22	27,35	19,60	20,40	3,42	2,30	1,22	0,41	100
FJ-19-4a_4	Fjallsendahraun	1,30	0,00	46,28	25,41	27,16	19,12	19,53	3,49	2,32	1,25	0,42	100
FJ-19-4a_5	Fjallsendahraun	0,00	0,85	47,28	25,42	26,93	20,35	19,04	3,47	2,33	1,21	0,40	100
FJ-19-4a_6	Fjallsendahraun	0,21	0,00	46,65	25,70	26,66	19,99	20,21	3,32	2,39	1,12	0,41	100
FJ-19-4a_7	Fjallsendahraun	0,45	0,00	47,22	25,23	27,32	19,90	20,10	3,16	2,31	1,14	0,38	100
FJ-19-4a_8	Fjallsendahraun	0,50	0,00	47,79	25,08	27,19	20,61	19,12	3,51	2,27	1,29	0,42	100
FJ-19-4a_9	Fjallsendahraun	0,64	0,00	47,10	24,70	27,18	19,91	20,22	3,38	2,34	1,24	0,39	100
FJ-19-4a_10	Fjallsendahraun	0,00	0,20	47,26	25,79	26,70	20,57	19,44	3,40	2,29	1,26	0,36	100
FJ-19-7a_1	Fjallsendahraun	0,19	0,00	46,68	25,44	25,01	21,67	19,74	3,62	2,41	1,54	0,37	100
FJ-19-7a_2	Fjallsendahraun	1,67	0,00	46,22	24,62	26,09	20,13	19,58	3,56	2,40	1,54	0,41	100
FJ-19-7a_3	Fjallsendahraun	0,91	0,00	46,50	24,87	24,81	21,69	19,79	3,59	2,41	1,48	0,44	100
FJ-19-7a_4	Fjallsendahraun	1,71	0,00	45,99	24,21	26,84	19,15	20,17	3,64	2,43	1,44	0,40	100
FJ-19-7a_5	Fjallsendahraun	1,89	0,00	45,44	24,60	26,40	19,04	19,98	3,71	2,42	1,49	0,46	100
FJ-19-7a_6	Fjallsendahraun	1,06	0,00	46,30	25,00	25,29	21,01	19,55	3,72	2,43	1,46	0,48	100
FJ-19-7a_7	Fjallsendahraun	1,99	0,00	45,91	23,48	26,74	19,16	20,54	3,69	2,42	1,55	0,44	100
FJ-19-7a_8	Fjallsendahraun	3,46	0,00	44,50	23,90	28,02	16,48	20,15	3,62	2,38	1,57	0,41	100
FJ-19-7a_9	Fjallsendahraun	1,22	0,00	46,58	24,15	26,13	20,45	20,15	3,64	2,42	1,45	0,38	100
FJ-19-7a_10	Fjallsendahraun	2,40	0,00	45,58	24,20	26,67	18,92	19,63	3,71	2,40	1,62	0,46	100
FJ-19-5b_1	Fjallsendahraun	0,00	1,51	47,28	24,25	26,06	21,22	19,31	3,37	2,40	1,31	0,57	100

FJ-19-5b_2	Fjallsendahraun	0,00	0,96	47,59	23,77	27,88	19,71	20,32	3,38	2,37	1,27	0,34	100
FJ-19-5b_3	Fjallsendahraun	0,00	0,64	46,87	25,42	26,09	20,79	19,27	3,57	2,37	1,39	0,46	100
FJ-19-5b_4	Fjallsendahraun	0,57	0,00	46,80	24,41	26,52	20,28	20,63	3,53	2,36	1,26	0,43	100
FJ-19-5b_5	Fjallsendahraun	0,00	0,00	47,09	25,16	26,31	20,78	20,09	3,51	2,34	1,36	0,45	100
FJ-19-5b_6	Fjallsendahraun	0,00	0,48	47,35	24,89	26,25	21,10	19,59	3,56	2,36	1,35	0,43	100
FJ-19-5b_7	Fjallsendahraun	0,35	0,00	46,85	24,71	25,78	21,06	20,51	3,45	2,36	1,24	0,53	100
FJ-19-5b_8	Fjallsendahraun	0,00	1,89	47,10	25,55	25,76	21,34	17,90	3,49	2,39	1,25	0,43	100
FJ-19-5b_9	Fjallsendahraun	0,02	0,00	46,87	25,24	26,22	20,65	20,24	3,59	2,39	1,29	0,37	100
FJ-19-5b_10	Fjallsendahraun	0,14	0,00	46,94	24,69	26,30	20,64	20,67	3,54	2,38	1,29	0,36	100
FJ-19-6a_1	Fjallsendahraun	0,44	0,00	46,93	24,44	26,60	20,33	20,74	3,35	2,38	1,26	0,46	100
FJ-19-6a_2	Fjallsendahraun	0,13	0,00	46,98	25,22	26,43	20,55	20,37	3,42	2,32	1,21	0,35	100
FJ-19-6a_3	Fjallsendahraun	3,75	0,00	44,27	22,98	29,33	14,95	21,39	3,45	2,35	1,33	0,47	100
FJ-19-6a_4	Fjallsendahraun	0,00	0,91	47,76	25,89	26,29	21,47	17,78	3,54	2,30	1,32	0,50	100
FJ-19-6a_5	Fjallsendahraun	0,06	0,00	47,34	24,06	27,21	20,14	21,10	3,34	2,37	1,26	0,48	100
FJ-19-6a_6	Fjallsendahraun	0,20	0,00	47,30	24,50	26,92	20,38	20,51	3,44	2,37	1,29	0,39	100
FJ-19-6a_7	Fjallsendahraun	1,12	0,00	45,90	25,43	27,16	18,74	19,93	3,51	2,32	1,28	0,50	100
FJ-19-6a_8	Fjallsendahraun	2,69	0,00	45,88	23,11	28,75	17,13	20,96	3,42	2,33	1,23	0,38	100
FJ-19-6a_9	Fjallsendahraun	1,71	0,00	45,91	23,95	28,27	17,64	21,23	3,28	2,35	1,22	0,35	100
FJ-19-6a_10	Fjallsendahraun	0,92	0,00	46,09	24,57	27,25	18,84	21,00	3,34	2,37	1,24	0,48	100
FJ-19-5a_1	Fjallsendahraun	0,00	0,25	47,35	24,94	25,82	21,53	19,73	3,52	2,35	1,43	0,42	100
FJ-19-5a_2	Fjallsendahraun	0,28	0,00	47,19	23,68	25,85	21,34	21,12	3,55	2,38	1,36	0,44	100
FJ-19-5a_3	Fjallsendahraun	0,00	0,69	46,97	25,33	26,33	20,64	19,29	3,46	2,37	1,44	0,44	100
FJ-19-5a_4	Fjallsendahraun	0,00	1,37	47,13	25,75	25,96	21,18	18,17	3,50	2,36	1,40	0,32	100
FJ-19-5a_5	Fjallsendahraun	0,18	0,00	46,66	25,47	26,38	20,28	20,09	3,48	2,36	1,37	0,38	100
FJ-19-5a_6	Fjallsendahraun	0,52	0,00	47,00	24,72	26,58	20,42	20,29	3,35	2,36	1,36	0,41	100
FJ-19-5a_7	Fjallsendahraun	0,46	0,00	46,86	24,91	26,22	20,65	20,24	3,46	2,35	1,28	0,44	100
FJ-19-5a_8	Fjallsendahraun	0,40	0,00	47,12	24,59	26,09	21,02	20,29	3,52	2,37	1,31	0,41	100
FJ-19-5a_9	Fjallsendahraun	0,18	0,00	46,96	24,36	26,76	20,20	20,93	3,49	2,36	1,34	0,39	100
FJ-19-9a_1	Fjallsendahraun	0,92	0,00	46,20	24,98	27,33	18,86	20,44	3,43	2,40	1,30	0,35	100

FJ-19-9a_2	Fjallsendahraun	4,15	0,00	43,66	21,76	31,14	12,52	22,82	3,53	2,40	1,28	0,40	100
FJ-19-9a_3	Fjallsendahraun	0,31	0,00	46,04	25,22	26,91	19,12	20,87	3,43	2,42	1,32	0,39	100
FJ-19-9a_4	Fjallsendahraun	0,19	0,00	47,04	24,73	26,74	20,30	20,65	3,42	2,36	1,26	0,36	100
FJ-19-9a_5	Fjallsendahraun	0,38	0,00	46,57	25,39	26,66	19,91	20,20	3,48	2,36	1,21	0,41	100
FJ-19-9a_6	Fjallsendahraun	0,68	0,00	46,41	25,23	26,74	19,67	19,82	3,57	2,43	1,43	0,43	100
FJ-19-9a_7	Fjallsendahraun	0,00	0,39	46,61	25,36	26,19	20,41	19,77	3,56	2,40	1,41	0,50	100
FJ-19-9a_8	Fjallsendahraun	2,43	0,00	45,87	23,55	28,18	17,70	20,76	3,37	2,33	1,25	0,43	100
FJ-19-9a_9	Fjallsendahraun	0,00	1,20	46,49	26,67	25,27	21,22	18,08	3,52	2,39	1,19	0,46	100
FJ-19-9a_10	Fjallsendahraun	0,17	0,00	46,79	25,21	27,08	19,71	20,47	3,44	2,39	1,19	0,34	100
FJ-19-3a_1	Fjallsendahraun	0,08	0,00	46,97	23,81	26,63	20,35	21,10	3,72	2,48	1,40	0,45	100
FJ-19-3a_2	Fjallsendahraun	2,15	0,00	45,98	23,44	28,49	17,48	20,98	3,55	2,33	1,21	0,37	100
FJ-19-3a_3	Fjallsendahraun	0,34	0,00	46,62	26,01	27,08	19,54	19,67	3,45	2,35	1,18	0,37	100
FJ-19-3a_4	Fjallsendahraun	0,00	0,72	47,09	26,13	26,70	20,39	18,64	3,40	2,32	1,32	0,38	100
FJ-19-3a_5	Fjallsendahraun	0,11	0,00	47,56	24,24	26,61	20,95	20,82	3,43	2,34	1,18	0,32	100
FJ-19-3a_6	Fjallsendahraun	0,68	0,00	45,30	24,17	26,26	19,04	21,67	3,60	2,68	1,49	0,41	100
FJ-19-3a_7	Fjallsendahraun	0,00	0,47	47,20	26,11	25,77	21,43	18,77	3,46	2,32	1,31	0,36	100
FJ-19-3a_8	Fjallsendahraun	0,34	0,00	46,30	25,53	26,67	19,63	20,32	3,50	2,36	1,19	0,45	100
FJ-19-3a_9	Fjallsendahraun	0,05	0,00	47,68	25,30	27,35	20,32	19,56	3,52	2,31	1,22	0,36	100
FJ-19-3a_10	Fjallsendahraun	0,00	1,64	47,58	25,74	26,29	21,29	17,58	3,45	2,38	1,25	0,38	100
FJ-19-10a_1	Fjallsendahraun	0,96	0,00	45,85	24,97	27,15	18,70	20,67	3,49	2,37	1,28	0,42	100
FJ-19-10a_2	Fjallsendahraun	0,75	0,00	46,60	23,63	27,48	19,12	21,53	3,43	2,39	1,33	0,34	100
FJ-19-10a_3	Fjallsendahraun	0,37	0,00	46,43	25,66	26,29	20,14	19,99	3,48	2,36	1,32	0,40	100
FJ-19-10a_4	Fjallsendahraun	1,70	0,00	44,89	25,29	27,54	17,35	20,29	3,59	2,39	1,37	0,48	100
FJ-19-10a_5	Fjallsendahraun	4,63	0,00	44,79	21,75	29,49	15,30	21,31	3,49	2,32	1,30	0,41	100
FJ-19-10a_6	Fjallsendahraun	0,63	0,00	46,21	25,88	26,98	19,23	19,70	3,51	2,35	1,28	0,44	100
FJ-19-10a_7	Fjallsendahraun	4,12	0,00	44,38	22,64	29,67	14,71	21,27	3,59	2,36	1,25	0,39	100
FJ-19-10a_8	Fjallsendahraun	1,03	0,00	45,75	25,66	27,03	18,72	19,94	3,55	2,34	1,28	0,46	100
FJ-19-10a_9	Fjallsendahraun	3,17	0,00	44,98	23,77	28,79	16,18	20,46	3,52	2,36	1,27	0,47	100
FJ-19-10a_10	Fjallsendahraun	2,05	0,00	45,30	24,18	28,33	16,97	20,77	3,60	2,36	1,24	0,52	100

FJ-19-10a_11	Fjallsendahraun	0,00	0,37	46,73	25,63	25,99	20,73	19,70	3,44	2,38	1,33	0,43	100
V2008-1a_1	Veiðivötn	2,55	0,00	45,41	23,62	26,95	18,47	20,06	3,97	2,44	1,47	0,48	100
V2008-1a_2	Veiðivötn	2,28	0,00	45,60	23,24	27,16	18,44	20,49	3,89	2,48	1,52	0,50	100
V2008-1a_3	Veiðivötn	2,19	0,00	44,65	24,40	26,32	18,33	20,50	3,54	2,52	1,64	0,56	100
V2008-1a_4	Veiðivötn	0,00	0,67	46,86	25,85	25,16	21,70	18,55	3,73	2,48	1,47	0,38	100
V2008-1a_5	Veiðivötn	1,96	0,00	45,41	23,83	27,29	18,12	20,49	3,91	2,50	1,51	0,39	100
V2008-1a_6	Veiðivötn	1,79	0,00	45,29	24,56	26,61	18,68	20,09	3,83	2,50	1,50	0,43	100
V2008-1a_7	Veiðivötn	0,23	0,00	47,14	23,22	25,30	21,84	21,32	3,79	2,51	1,39	0,39	100
V2008-1a_8	Veiðivötn	3,19	0,00	44,37	23,39	28,70	15,66	20,75	3,86	2,53	1,55	0,36	100
V2008-1a_9	Veiðivötn	3,34	0,00	45,18	22,19	27,62	17,56	21,17	3,75	2,47	1,50	0,40	100
V2008-1a_10	Veiðivötn	1,58	0,00	45,69	24,65	26,34	19,35	19,89	3,80	2,48	1,45	0,45	100
TJ-2008-1_1	Tjörvahraun	6,11	0,00	51,39	4,94	21,05	30,34	19,62	4,26	1,97	10,98	0,72	100
TJ-2008-1_2	Tjörvahraun	4,23	0,00	52,35	7,27	19,49	32,86	18,90	4,26	2,04	10,22	0,72	100
TJ-2008-1_3	Tjörvahraun	6,51	0,00	50,78	10,14	22,13	28,65	17,01	4,40	1,97	8,44	0,74	100
TJ-2008-1_4	Tjörvahraun	6,48	0,00	51,56	4,18	21,74	29,82	20,85	4,15	2,05	9,94	0,80	100
TJ-2008-1_5	Tjörvahraun	3,08	0,00	52,54	11,40	20,07	32,47	16,97	4,09	1,99	9,13	0,80	100
TJ-2008-1_6	Tjörvahraun	6,87	0,00	51,19	4,13	21,97	29,22	20,48	4,22	2,03	10,24	0,85	100
TJ-2008-1_7	Tjörvahraun	5,44	0,00	51,36	5,05	20,95	30,40	19,98	4,25	2,03	11,13	0,77	100
TJ-2008-1_8	Tjörvahraun	10,82	0,00	47,64	10,02	30,46	17,18	19,40	4,03	2,05	5,25	0,79	100
TJ-2008-1_9	Tjörvahraun	4,29	0,00	51,82	11,15	20,84	30,98	17,27	3,92	2,02	8,85	0,69	100
VO-2008-2_1	Vatnaöldur	0,92	0,00	47,03	25,26	27,69	19,33	19,31	3,57	2,35	1,30	0,26	100
VO-2008-2_2	Vatnaöldur	1,36	0,00	46,96	23,93	28,07	18,89	20,22	3,54	2,34	1,26	0,38	100
VO-2008-2_3	Vatnaöldur	2,48	0,00	45,10	23,28	29,21	15,90	21,34	3,53	2,41	1,41	0,44	100
VO-2008-2_4	Vatnaöldur	1,89	0,00	45,94	24,71	27,21	18,73	19,84	3,55	2,32	1,31	0,44	100
VO-2008-2_5	Vatnaöldur	0,34	0,00	47,08	25,67	27,01	20,07	19,38	3,55	2,38	1,26	0,35	100
VO-2008-2_6	Vatnaöldur	1,18	0,00	47,04	24,83	27,88	19,16	19,40	3,53	2,33	1,29	0,40	100
VO-2008-2_7	Vatnaöldur	2,18	0,00	46,15	23,56	28,89	17,26	20,55	3,50	2,35	1,27	0,44	100
TR-2008-3b_1	Tröllahraun	0,21	0,00	47,82	25,18	27,50	20,32	19,41	3,46	2,32	1,22	0,37	100
TR-2008-3b_2	Tröllahraun	1,17	0,00	47,79	22,36	27,37	20,42	21,26	3,52	2,32	1,22	0,35	100

TR-2008-3b_3	Tröllahraun	0,00	0,78	47,47	25,46	26,92	20,55	18,78	3,48	2,33	1,29	0,42	100
TR-2008-3b_4	Tröllahraun	0,33	0,00	47,45	25,34	26,47	20,98	19,38	3,54	2,35	1,13	0,48	100
TR-2008-3b_5	Tröllahraun	0,01	0,00	47,79	24,87	26,80	20,99	19,97	3,38	2,37	1,23	0,38	100
TR-2008-3b_6	Tröllahraun	0,00	0,00	47,01	24,87	26,82	20,18	20,65	3,42	2,37	1,27	0,42	100
TR-2008-3b_7	Tröllahraun	0,14	0,00	47,55	24,47	26,29	21,25	20,11	3,65	2,37	1,28	0,43	100
TR-2008-3b_8	Tröllahraun	0,33	0,00	47,27	24,91	27,37	19,90	20,04	3,47	2,35	1,26	0,37	100
TR-2008-2_1	Tröllahraun	0,28	0,00	47,81	24,47	27,20	20,60	19,95	3,58	2,30	1,23	0,38	100
TR-2008-2_2	Tröllahraun	0,47	0,00	46,69	24,38	27,97	18,72	20,98	3,43	2,35	1,29	0,41	100
TR-2008-2_3	Tröllahraun	0,00	0,88	47,14	25,57	26,53	20,61	18,95	3,49	2,35	1,23	0,39	100
TR-2008-2_4	Tröllahraun	0,21	0,00	47,38	25,96	27,26	20,12	19,07	3,50	2,25	1,26	0,38	100
TR-2008-2_5	Tröllahraun	0,45	0,00	47,19	25,51	27,50	19,68	19,40	3,45	2,28	1,32	0,40	100
TR-2008-2_6	Tröllahraun	0,29	0,00	47,07	25,59	26,94	20,13	19,64	3,42	2,35	1,26	0,39	100

Appendix E

Table 7: *OPAM thermobarometry calculations, using the same method as Hartley et al., 2018.*

Sample	Locality	Pressure [kbar]
FJ-19-1a_7	Fjallsendahraun	2,26
FJ-19-2a_2	Fjallsendahraun	1,95
FJ-19-2a_4	Fjallsendahraun	1,57
FJ-19-3a_5	Fjallsendahraun	2,37
FJ-19-3a_7	Fjallsendahraun	1,24
FJ-19-3a_8	Fjallsendahraun	1,73
FJ-19-5a_1	Fjallsendahraun	1,73
FJ-19-5a_2	Fjallsendahraun	2,39
FJ-19-5a_3	Fjallsendahraun	1,85
FJ-19-5a_4	Fjallsendahraun	1,82
FJ-19-5a_9	Fjallsendahraun	2,36
FJ-19-5b_1	Fjallsendahraun	2,60
FJ-19-5b_3	Fjallsendahraun	1,79
FJ-19-5b_4	Fjallsendahraun	1,97
FJ-19-5b_6	Fjallsendahraun	1,95
FJ-19-5b_7	Fjallsendahraun	1,77
FJ-19-5b_8	Fjallsendahraun	2,12
FJ-19-5b_9	Fjallsendahraun	1,82
FJ-19-5b_10	Fjallsendahraun	2,11
FJ-19-6a_2	Fjallsendahraun	1,94
FJ-19-7a_1	Fjallsendahraun	1,17

Sample	Locality	Pressure [kbar]
FJ-19-7a_3	Fjallsendahraun	0,94
FJ-19-9a_3	Fjallsendahraun	1,98
FJ-19-9a_4	Fjallsendahraun	2,11
FJ-19-9a_7	Fjallsendahraun	1,81
FJ-19-9a_9	Fjallsendahraun	1,24
FJ-19-10a_3	Fjallsendahraun	1,41
FJ-19-10a_11	Fjallsendahraun	1,67
V2008-1a_7	Veiðivötn	2,40
TR-2008-2_3	Tröllahraun	1,89
Vc1_glass4	Veiðivötn center	1,19
Vc3_glass10	Veiðivötn center	1,76
Vc3_glass19	Veiðivötn center	2,01
Vc_G5 spot3	Veiðivötn center	1,26
Vc_G4 spot2	Veiðivötn center	1,25
Vc_G4 spot3	Veiðivötn center	1,60
Vs3_glass37	Veiðivötn south	1,92
Vs2_glass37	Veiðivötn south	1,76
Vs3_glass39	Veiðivötn south	1,35
Vs_G2 spot1	Veiðivötn south	1,09
S36	Holuhraun II	2,35
S36	Holuhraun II	1,57

S36	Holuhraun II	1,08
S36	Holuhraun II	1,26
PKT77B	Holuhraun III	1,35
PKT77B	Holuhraun III	0,73
PKT77B	Holuhraun III	1,59
PKT77B	Holuhraun III	1,14
PKT77B	Holuhraun III	1,36
PKT77B	Holuhraun III	0,71
PKT77B	Holuhraun III	0,84
PKT77B	Holuhraun III	0,46
PKT77B	Holuhraun III	1,78
PKT77B	Holuhraun III	1,75
PKT77B	Holuhraun III	1,51
PKT77B	Holuhraun III	0,77
PKT77C	Holuhraun III	1,50
PKT77C	Holuhraun III	1,36
JPR030914-04	Holuhraun III	1,80
JPR030914-05	Holuhraun III	1,06
JPR030914-07	Holuhraun III	1,29
JPR030914-08	Holuhraun III	1,52
JPR030914-09	Holuhraun III	1,76
JS040914-07	Holuhraun III	1,22
JS040914-08	Holuhraun III	1,15
JS040914-09	Holuhraun III	1,44
JS040914-10	Holuhraun III	1,00
JS040914-12	Holuhraun III	0,76
JS040914-13	Holuhraun III	0,84
JS040914-14	Holuhraun III	0,91
JS040914-15	Holuhraun III	0,85

JS040914-17	Holuhraun III	1,11
JS040914-18	Holuhraun III	1,03
JS040914-19	Holuhraun III	0,79
JS040914-20	Holuhraun III	0,46
JS040914-21	Holuhraun III	1,10
JS040914-07b	Holuhraun III	2,95
JS040914-07b	Holuhraun III	2,80
JS040914-07b	Holuhraun III	2,83
JS040914-07b	Holuhraun III	2,60
JS040914-07b	Holuhraun III	3,35
JS040914-07b	Holuhraun III	3,21
JS040914-07b	Holuhraun III	2,46
JS040914-07b	Holuhraun III	3,00
JS040914-07b	Holuhraun III	2,08
07092014 Pele	Holuhraun III	2,20
07092014 Pele	Holuhraun III	1,50
07092014 Pele	Holuhraun III	2,49
07092014 Pele	Holuhraun III	2,48
PAO07092016	Holuhraun III	2,75
PAO07092017	Holuhraun III	2,73
PAO07092020	Holuhraun III	2,18
PAO07092022	Holuhraun III	3,28
PAO07092024	Holuhraun III	2,78
PAO07092025	Holuhraun III	2,78
JAS130915	Holuhraun III	2,51
JAS130917	Holuhraun III	3,06
JAS130918	Holuhraun III	3,30
JAS130920	Holuhraun III	2,96
JAS130921	Holuhraun III	2,28

JAS130923	Holuhraun III	2,64
JAS130924	Holuhraun III	2,61
JAS130925	Holuhraun III	2,38
JAS130926	Holuhraun III	2,66
JAS130927	Holuhraun III	2,20
JAS130928	Holuhraun III	2,58
AH170914-04	Holuhraun III	1,75
AH170914-05	Holuhraun III	2,14
AH170914-06	Holuhraun III	2,01
AH170914-10	Holuhraun III	2,49
AH170914-14	Holuhraun III	2,26
AH170914-15	Holuhraun III	2,43
BAO200914-02	Holuhraun III	2,33
BAO200914-03	Holuhraun III	2,97
BAO200914-04	Holuhraun III	2,62
BAO200914-05	Holuhraun III	3,12
BAO200914-07	Holuhraun III	2,62
BAO200914-08	Holuhraun III	2,75
BAO200914-09	Holuhraun III	2,47
BAO200914-10	Holuhraun III	1,61
BAO200914-11	Holuhraun III	2,74
BAO200914-12	Holuhraun III	3,38
BAO200914-15	Holuhraun III	3,27
BAO200914-16	Holuhraun III	3,02
TTJIJ081014	Holuhraun III	2,17
TTJIJ081015	Holuhraun III	2,35
TTJIJ081016	Holuhraun III	2,48
TTJIJ081017	Holuhraun III	1,79
TTJIJ081018	Holuhraun III	2,39

TTJIJ081019	Holuhraun III	1,96
TTJIJ081020	Holuhraun III	2,41
TTJIJ081021	Holuhraun III	2,40
TTJIJ081022	Holuhraun III	2,35
TTJIJ081023	Holuhraun III	2,05
TTJIJ081024	Holuhraun III	2,74
TTJIJ081025	Holuhraun III	2,26
TTJIJ081026	Holuhraun III	2,16
TTJIJ081027	Holuhraun III	2,44
TTJIJ081028	Holuhraun III	1,73
MSR291014	Holuhraun III	1,60
MSR291015	Holuhraun III	1,95
MSR291016	Holuhraun III	1,92
MSR291018	Holuhraun III	2,24
MSR291019	Holuhraun III	2,46
MSR291020	Holuhraun III	2,74
MSR291021	Holuhraun III	2,50
MSR291022	Holuhraun III	2,53
MSR291024	Holuhraun III	2,74
MSR291025	Holuhraun III	2,54
MSR291026	Holuhraun III	2,28
MSR291027	Holuhraun III	2,61
MSR291028	Holuhraun III	2,43
MSR291014-3	Holuhraun III	1,89
MSR291014-5	Holuhraun III	1,76
MSR291014-6	Holuhraun III	1,73
MSR291014-7	Holuhraun III	1,56
MSR291014-8	Holuhraun III	1,87
MSR291014-9	Holuhraun III	2,30

MSR291014-10	Holuhraun III	1,87
MSR291014-11	Holuhraun III	1,64
MSR291014-12	Holuhraun III	1,93
MSR291014-13	Holuhraun III	2,58

MSR291014-14	Holuhraun III	1,48
MSR291014-15	Holuhraun III	2,22
MSR291014-16	Holuhraun III	2,09
MSR291014-17	Holuhraun III	1,76